

Direct Experiments of Neutron Capture on Stable and Unstable Isotopes for Stellar Nucleosynthesis Studies

Jorge Lerendegui-Marco^{1,*} , Javier Balibrea-Correa¹, Victor Babiano-Suarez¹, César Domingo-Pardo¹, Gabriel de la Fuente-Rosales¹, Bernardo Gameiro¹, Ion Ladarescu¹, Ariel Tarifeño-Saldivia¹, Pablo Torres-Sánchez¹, Oliver Aberle², Victor Alcayne³, Simone Amaducci⁴, Michael Bacak⁵, Jesús Bartolomé⁶, Aparna Basavaraja-Allannavar⁷, Ana-Paula Bernardes², Eric Berthoumieux⁸, Roland Beyer⁹, Matthew Birch¹⁰, Selin Birincioglu¹¹, Marian Boromiza¹², Damir Bosnar¹³, Benedetta Brusasco⁷, Manuel Caamaño¹⁴, Aline Cahuzac⁸, Francisco Calviño⁷, Marco Calviani², Daniel Cano-Ott³, Adrià Casanovas⁷, Donato Castelluccio^{15,16}, Francesco Cerutti², Gabriele Cescutti^{17,18}, Enrico Chiaveri^{2,10}, Gerardo Claps¹⁹, Paolo Colombetti^{20,21}, Nicola Colonna²², Patrizio Console Camprini^{15,16}, Guillem Cortés⁷, Miguel Cortés-Giraldo⁶, Luigi Cosentino⁴, Sergio Cristallo^{23,24}, Angelica D'Ottavi¹⁰, Maria Diakaki²⁵, Mario Di Castro², Augusto Di Chicco²⁶, Mirco Dietz²⁶, Emeric Dupont⁸, Ignacio Durán¹⁴, Zinovia Eleme²⁷, Sylvain Fargier², Martin Farkas², Beatriz Fernández-Domínguez¹⁴, Paolo Finocchiaro⁴, Will Flanagan²⁸, Varvara Foteinou²⁷, Valter Furman²⁹, Aman Gandhi¹², Francisco García-Infantes¹¹, Aleksandra Gawlik-Ramiega³⁰, Gianpiero Gervino^{20,21}, Simone Gilardoni², Enrique González-Romero³, Styliani Goula^{27,2}, Erich Griesmayer⁵, Carlos Guerrero⁶, Frank Gunsing⁸, Carlo Gustavino³¹, Jan Heyse³², William Hillman¹⁰, Elizabeth Jacoby²⁸, David Jenkins³³, Erwin Jericha⁵, Arnd Junghans⁹, Ulli Köster³⁴, Yacine Kadi², Nasser Kalantar-Nayestanaki³⁵, Kalliopi Kaperoni²⁵, Myroslav Kavatsyuk³⁵, Michael Kokkoris²⁵, Sotirios Kopanos²⁵, Yury Kopatch²⁹, Milan Krtička³⁶, Nikolaos Kyritsis²⁵, Claudia Lederer-Woods¹¹, Giuseppe Lorusso³⁷, Alice Manna², Trinitario Martínez³, Marco Martínez-Cañada³⁸, Alessandro Masi², Cristian Massimi^{16,39}, Pierfrancesco Mastinu⁴⁰, Mario Mastromarco^{22,41}, Emilio-Andrea Maugeri⁴², Annamaria Mazzone^{22,43}, Emilio Mendoza³, Alberto Mengoni^{15,16}, Veatriki Michalopoulou²⁵, Paolo Milazzo¹⁷, Jacob Moldenhauer²⁸, Riccardo Mucciola²², Elizabeth Musacchio González⁴⁰, Agatino Musumarra^{44,45}, Alexandru Negret¹², Emmanuel Odusina¹¹, Dimitrios Papanikolaou⁴⁴, Carlos Paradela³², Albert Parmenter²⁸, Nikolas Patronis²⁷, José Antonio Pavón⁶, Maria Pellegriti⁴⁴, Pablo Pérez-Maroto⁷, Alberto Pérez de Rada Fiol³, Giulio Peretto²², Jarosław Perkowski³⁰, Cristina Petrone¹², Nicholas Pieretti^{16,39}, Luciano Piersanti^{23,24}, Elisa Pirovano²⁶, Ignacio Porras³⁸, Javier Praena³⁸, José-Manuel Quesada⁶, René Reifarth⁴⁶, Alejandro Reina⁶, Dimitri Rochman⁴², Yuriy Romanets⁴⁷, Annie Rooney¹¹, Gerard Rovira⁴⁸, Carlo Rubbia², Adrián Sánchez-Caballero³, Nicolás Sánchez-Vázquez¹⁴, Rudra Sahoo¹⁶, Salma²², Daniele Scarpa⁴⁰, Gavin Smith¹⁰, Nikolay Sosnin¹⁰, Michele Spelta^{17,18}, Krzysztof Stasiak³⁰, Giuseppe Tagliente²², Antonella Tamburrino¹⁹, Diego Tarrío⁴⁹, Giorgios Tsiledakis⁸, Stanislav Valenta³⁶, Pedro Vaz⁴⁷, Gianfranco Vecchio⁴, Diego Vescovi^{23,24}, Vasilis Vlachoudis², Rosa Vlastou²⁵, Anton Wallner⁹, Christina Weiss⁵, Tobias Wright¹⁰, Renjie Wu³³, Roberto Zarrella¹⁶, Petar Žugec¹³

¹ Instituto de Física Corpuscular, CSIC - Universidad de Valencia, Spain

² European Organization for Nuclear Research (CERN), Switzerland

³ Centro de Investigaciones Energéticas Medioambientales y Tecnológicas (CIEMAT), Spain

⁴ INFN Laboratori Nazionali del Sud, Catania, Italy

⁵ TU Wien, Atominstitut, Stadionallee 2, 1020 Wien, Austria

⁶ Universidad de Sevilla, Spain

⁷ Universitat Politècnica de Catalunya, Spain

⁸ CEA Irfu, Université Paris-Saclay, F-91191 Gif-sur-Yvette, France

⁹ Helmholtz-Zentrum Dresden-Rossendorf, Germany

¹⁰ University of Manchester, United Kingdom

¹¹ School of Physics and Astronomy, University of Edinburgh, United Kingdom

¹² Horia Hulubei National Institute of Physics and Nuclear Engineering, Romania

¹³ Department of Physics, Faculty of Science, University of Zagreb, Zagreb, Croatia

¹⁴ University of Santiago de Compostela, Spain

¹⁵ Agenzia nazionale per le nuove tecnologie, l'energia e lo sviluppo economico sostenibile (ENEA), Italy

¹⁶ Istituto Nazionale di Fisica Nucleare, Sezione di Bologna, Italy

¹⁷ Istituto Nazionale di Fisica Nucleare, Sezione di Trieste, Italy



Received:

Revised:

Accepted:

Published:

Copyright: © 2026 by the authors.

Licensee MDPI, Basel, Switzerland.

This article is an open access article

distributed under the terms and

conditions of the [Creative Commons](https://creativecommons.org/licenses/by/4.0/)

[Attribution \(CC BY\) license](https://creativecommons.org/licenses/by/4.0/).

- 18 Department of Physics, University of Trieste, Italy
19 INFN Laboratori Nazionali di Frascati, Italy
20 Istituto Nazionale di Fisica Nucleare, Sezione di Torino, Italy
21 Department of Physics, University of Torino, Italy
22 Istituto Nazionale di Fisica Nucleare, Sezione di Bari, Italy
23 Istituto Nazionale di Fisica Nucleare, Sezione di Perugia, Italy
24 Istituto Nazionale di Astrofisica - Osservatorio Astronomico d' Abruzzo, Italy
25 National Technical University of Athens, Greece
26 Physikalisch-Technische Bundesanstalt (PTB), Bundesallee 100, 38116 Braunschweig, Germany
27 University of Ioannina, Greece
28 University of Dallas, USA
29 Affiliated with an institute covered by a cooperation agreement with CERN
30 University of Lodz, Poland
31 Istituto Nazionale di Fisica Nucleare, Sezione di Roma1, Roma, Italy
32 European Commission, Joint Research Centre (JRC), Geel, Belgium
33 University of York, United Kingdom
34 Institut Laue-Langevin, 71 Avenue des Martyrs, 38042, Grenoble, France
35 University of Groningen, NL-9747 AA Groningen, the Netherlands
36 Charles University, Prague, Czech Republic
37 National Physical Laboratory, Hampton Road, Teddington, UK
38 University of Granada, Spain
39 Dipartimento di Fisica e Astronomia, Università di Bologna, Italy
40 INFN Laboratori Nazionali di Legnaro, Italy
41 Dipartimento Interateneo di Fisica, Università degli Studi di Bari, Italy
42 Paul Scherrer Institut (PSI), Villigen, Switzerland
43 Consiglio Nazionale delle Ricerche, Bari, Italy
44 Istituto Nazionale di Fisica Nucleare, Sezione di Catania, Italy
45 Department of Physics and Astronomy, University of Catania, Italy
46 Goethe University Frankfurt, Germany
47 Instituto Superior Técnico, Lisbon, Portugal
48 Japan Atomic Energy Agency (JAEA), Tokai-Mura, Japan
49 Department of Physics and Astronomy, Uppsala University, Box 516, 75120 Uppsala, Sweden
* Correspondence: jorge.lerendegui@ific.uv.es

Abstract

Neutron-capture reactions provide essential nuclear-physics input for modeling the synthesis of heavy elements in stars. The growing precision of stellar spectroscopy and isotopic measurements in presolar SiC grains now demands cross sections with improved accuracy over the full energy range, and access to unstable nuclei relevant to slow (s-) process branchings and the intermediate (i-) process. This article reviews recent progress in direct neutron-capture measurements, focusing on time-of-flight (TOF) experiments at CERN n_TOF and complementary activation techniques. Substantial advances have been achieved for stable s-only and bottleneck isotopes, significantly improving constraints on s-process models. In parallel, the combination of high instantaneous neutron fluxes and advanced detector systems has facilitated first-time measurements of several radioactive branching-point nuclei. Feasibility studies, however, reveal current limitations related to sample availability, background conditions, and restricted energy coverage. In this context, the complementarity between TOF and activation emerges as a central strategy. Future developments, including high-flux facilities and novel inverse-kinematics experiments in ion storage rings, are expected to extend the boundaries of neutron-capture measurements, overcoming current limitations and helping to unlock new frontiers in our understanding of stellar nucleosynthesis.

Keywords: direct neutron capture; s-process; i-process; nuclear astrophysics; CERN n_TOF; time-of-flight; activation

1. Introduction

One of the most active research areas in nuclear astrophysics is the study of the nucleosynthesis of heavy elements ($A \gtrsim 60$) in the universe. The production of these elements is primarily governed by neutron-capture processes, which play a fundamental role in shaping the observed abundance distribution of nuclei heavier than iron. The involved mechanisms, first presented in detail in the works of Burbidge [1] and Cameron [2] almost 70 years ago, are characterized by different neutron densities of the astrophysical environment which lead to different relative timescales of neutron capture and β -decay.

The rapid neutron-capture process (r-process) occurs in explosive astrophysical environments, characterized by extremely high neutron densities ($N_n > 10^{20} \text{ cm}^{-3}$), such as supernovae or neutron-star mergers. Under these conditions, successive neutron captures proceed much faster than β -decay, producing highly neutron-rich nuclei located far from the valley of stability. In contrast, the slow neutron-capture process (s-process) operates in stellar environments with relatively low neutron densities ($N_n \approx 10^6 - 10^{12} \text{ cm}^{-3}$), such as asymptotic giant branch (AGB) stars during the late stages of stellar evolution [3]. In this case, neutron capture occurs on timescales longer than or comparable to β -decay, and nucleosynthesis proceeds along the valley of stability through a sequence of neutron captures and β -decays, gradually producing heavier nuclei up to bismuth. This process is, together with the r-process, responsible for the production of the majority ($\approx 99\%$) of the observed solar abundances of elements heavier than iron (see e.g. Fig. 1 of Ref [4]). More recently, an intermediate neutron-capture process (i-process), originally proposed by Cowan and Rose in 1977 [5], has been identified. This process occurs under neutron densities intermediate between those of the s- and r-processes ($N_n \approx 10^{13} - 10^{16} \text{ cm}^{-3}$) and involves nuclei located only a few mass units away from stability. The i-process has been shown to play an important role in explaining the abundance patterns observed in certain low-metallicity AGB stars and carbon-enhanced metal-poor stars [6].

From the experimental nuclear physics perspective, the key ingredient to improve the nucleosynthesis models is the accurate determination of neutron-capture cross sections at all relevant energies. This article reviews recent developments in direct neutron-capture measurements relevant to s-process nucleosynthesis in AGB and massive stars [3,7]. As described in Sec. 2, two different methodologies for neutron-capture cross-section measurements have been extensively applied so far in many laboratories worldwide, neutron time-of-flight (TOF) and neutron activation, thereby covering more than 300 s-process involved nuclei, most of them stable [4,8]. Despite the extensive experimental activities, there are still significant needs for new measurements, as discussed in Sec. 3. Sec. 4 discusses the recent efforts at CERN n_TOF to expand the experimental knowledge on direct neutron capture cross section. The main limitations of current state-of-the-art TOF experiments and the recent advances on both the TOF and activation techniques [3] at CERN n_TOF are then discussed in Sec. 5. Lastly, Sec. 6 presents future ideas to complement the existing methodologies with new measuring stations and techniques.

2. Experimental methods for direct neutron capture measurements

In an astrophysical environment where nucleosynthesis occurs, the stellar plasma is characterized by a temperature T at which particles are in thermodynamic equilibrium and their energies follow a Maxwell-Boltzmann distribution. Consequently, the quantity of astrophysical relevance is the neutron-induced cross section averaged over this stellar neutron-energy distribution, commonly referred to as the Maxwellian-averaged cross section (MACS) [9]. The latter has been compiled for s-process temperatures, $kT = 5 - 100 \text{ keV}$, in the KADoNiS v0.3 database [10]. Fig. 1 shows the example of the $^{171}\text{Tm}(n,\gamma)$ cross section compared to the Maxwell-Boltzmann energy distribution at the reference

temperature $kT = 30$ keV (hereafter MACS_{30}) to illustrate the contribution of different energy ranges of the neutron capture cross section to the stellar capture rate.

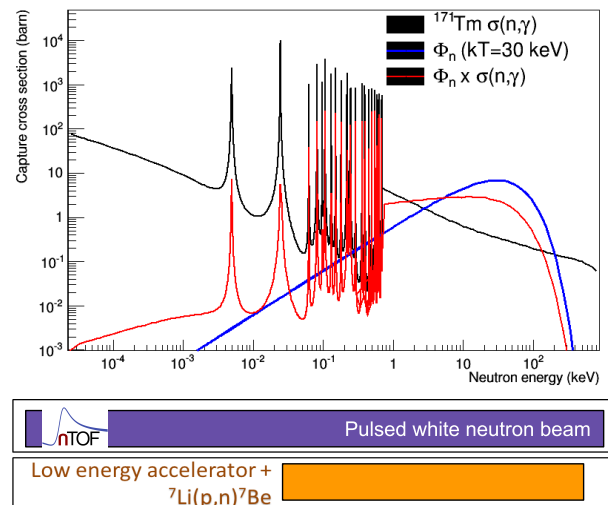


Figure 1. Top: Maxwell-Boltzmann spectrum of neutrons at the reference stellar temperature $kT = 30$ keV (blue curve), example of an (n,γ) cross section as available in JEFF-3.3 (black curve) and the convolution of the two (red curve), illustrating the contribution to the MACS. The units in the vertical axis are relevant only for the cross section. Bottom: Energy range covered by the two mostly employed beams and techniques for stellar (n,γ) measurements (see text for details).

Experimentally, neutron-capture cross sections relevant to stellar nucleosynthesis can be measured with direct methods using two complementary approaches: activation and time-of-flight (TOF) techniques. On the one hand, TOF facilities based today on spallation neutron sources produce white neutron spectra covering a broad neutron energy range. Combined with precise neutron-energy determination through the time-of-flight method, these facilities allow measurement of energy-dependent cross sections over a wide range of neutron energies, from which MACS values can be derived for astrophysical relevant temperatures. Neutron capture measurements for astrophysics are carried out in different white-neutron beam facilities across the world, such as GELINA [11], LANSCE [12], AN-NRI [13], Back-n [14] or n_TOF [15,16]. Sec. 4 will focus on the latter and review some of the recent highlights on neutron capture measurements of astrophysical relevance.

Neutron-capture TOF experiments are sometimes limited by the quality (isotopic enrichment) and quantity of sample material available for the experiment. This is particularly critical for the case of unstable isotopes, such as the s-process branching points [17]. Alternatively, in activation experiments, samples are irradiated with neutron spectra resembling stellar neutron distributions, allowing direct determination of MACS values at specific temperatures. As indicated in the bottom panel of Fig. 1, a quasi-stellar neutron spectrum at $kT = 25$ keV can be obtained using a low-energy proton accelerator and the $^7\text{Li}(p,n)^7\text{Be}$ reaction [18]. An intense research program on direct (n,γ) activation measurements for astrophysics has been carried out in facilities like FZK [19], LiLiT-SARAF [20], HISPANoS-CNA [21] or LeNoS-LNL [22].

The activation technique in world-leading facilities in terms of neutron flux, FZK [18, 19] and LiLiT-SARAF [23], has shown an unsurpassed sensitivity for the measurement of sub-microgram samples (i.e. 10^{14} atoms) [19] and can be the only direct method for cases where the high sample-decay induced background would represent an important limitation for the TOF measurement (see Sec. 4). On the contrary, activation in quasi-stellar beams has been typically limited to a single accessible stellar temperature ($kT = 25$ keV). Several facilities have studied methodologies to tune the outgoing neutron spectrum by

modifying the proton energy and sample angle [22,24,25], using ring-shaped sample to access lower s-process temperatures [26] or combining multiple proton energies to access higher temperatures ($kT = 90\text{keV}$) found in massive stars [27].

With the two-fold aim of covering a wider range and enabling direct measurement of low mass samples, mainly of unstable species not accessible via TOF, a new generation of high-flux neutron-activation stations with tuneable energy range has been proposed at CERN [28,29], as it is presented in Secs. 5 and 6.

3. Data needs for stable and unstable isotopes

Despite the extensive experimental activities over the last decades, there are still acute needs for new neutron-capture cross-section measurements, and for a large number of the measured isotopes improvements are required both in the covered energy range (approximately from 1 eV up to 100 keV) and in the obtained accuracy. Related to the latter, many previous measurements present cross-section uncertainties that are significantly larger than the 5% attainable in the measured abundance ratios from meteorite grains [3]. The values of MACS_{30} for all the nuclei involved in the s-process pathway and their current uncertainties are depicted in Fig. 2. Among all the isotopes plotted in this figure, several groups of key nuclei can be distinguished which have a crucial impact on the nucleosynthesis process [4,8,30]. An accurate knowledge of their stellar capture rate is indispensable for a better understanding of the neutron economy in the s-process and the resulting calculated abundances. The present status and needs for these particularly relevant isotopes are summarized in Table 1.

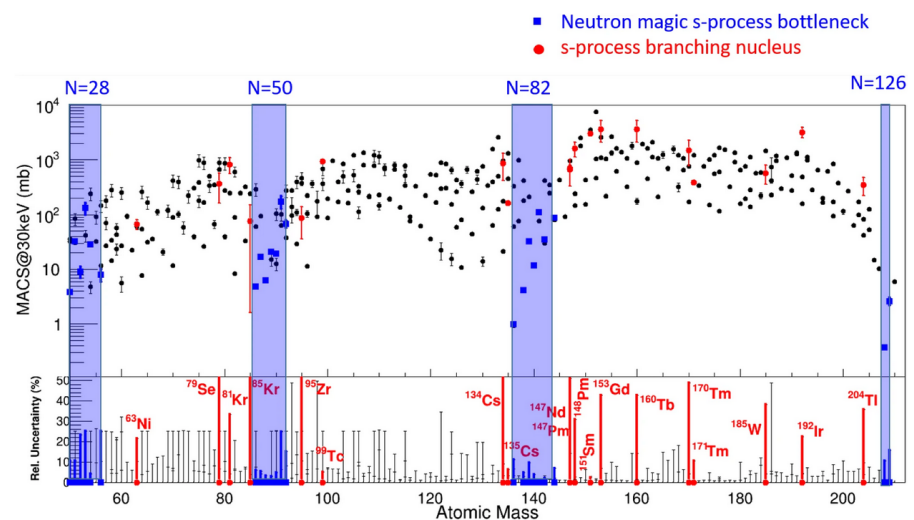


Figure 2. MACS_{30} in KADoNis v0.3 [10] (top) and their present accuracy (bottom). Nuclei acting as s-process bottlenecks and branching points are displayed in blue and red, respectively. Figure taken from Ref. [30].

The first family of key isotopes are the s-only isotopes, nuclei which are solely produced by the s-process since they are blocked from r-process contributions by other stable isobars. The s-only abundances serve as a benchmark for the nucleosynthesis and galactic-chemical evolution models. The MACS of the s-only nuclei are known with few exceptions within the required 5% or even down to 2%. A complete list of the 33 s-only isotopes and their current uncertainties can be found in Ref [4].

Further, nuclei located in neutron shell-closures, characterized by small capture cross sections (see Fig. 2), act as s-process bottlenecks. The s-process flow gives rise to the three characteristic abundance peaks at the neutron-shell closures. These elements — Sr, Y, Zr ($N = 50$), Ba, La, Ce, Nd, Sm ($N = 82$) and Pb, Bi ($N = 126$)— show-up prominently in

spectroscopic observations of stellar atmospheres and thus, they represent a sensitive probe for stellar models. However, as a consequence of their small cross sections, experimental uncertainties are still large (even higher than 10%) for some neutron-magic nuclei [4,8].

Particular attention has also been given to unstable nuclei acting as branching points in the s-process, highlighted in red in Fig. 2. At these nuclei, featuring relatively long half-lives (years), neutron capture and β -decay compete, leading to a branching of the nucleosynthesis path [3]. The resulting isotopic abundance patterns are highly sensitive to the physical conditions of the stellar environment, such as temperature and neutron density. Therefore, precise measurements of neutron-capture cross sections at branching points, combined with abundance observations and stellar models, provide valuable constraints on stellar evolution and nucleosynthesis conditions.

Despite their relevance, only a small fraction of the key s-process branching nuclei listed in [3] have been measured with high accuracy to date [17,30] and there is still a significant number of them that have not been accessed owing to several experimental limitations. The latter comprise the difficulty to produce samples of these isotopes in sizable amounts with a high enough enrichment. Furthermore, their activity implies a considerable radiation hazard and represents an intense source of background. As discussed in Sec. 4, a combined effort has been carried out during the last decade between Institut Laue-Langevin (ILL)-Grenoble (France) and Paul Scherrer Institute (PSI)-Villigen (Switzerland) to produce high quality samples of these nuclei to measure the neutron capture cross section via TOF at CERN n_TOF [31].

Table 1. Summary of data needs on direct (n,γ) measurements for key isotopes for stellar nucleosynthesis studies.

Process	Group of nuclei	Challenge	Status	Main need
s-process	s-only isotopes	Required accuracy	Unc. $\geq 5\%$ (e.g. $^{80,82}\text{Kr}$, ^{198}Hg)	Higher accuracy
s-process	bottlenecks	Small σ	Unc. $\geq 10\%$ (e.g. ^{208}Pb)	Higher sensitivity
s-process	branching points	Low mass, activity background	Few measured	Higher flux
i-process	See e.g. Refs. [32–34]	Short-lived unstable	No data	New concepts (See Sec. 6)

Lastly, neutron-capture reactions on radioactive isotopes also play a crucial role in the i-process nucleosynthesis. The reaction flow of the i-process travels through radioactive nuclei 2–6 units away from stability on the neutron-rich side, where no experimental data from direct neutron capture cross sections are available to date. Recent Monte Carlo sensitivity studies [32–34] have identified relevant neutron capture reactions which significantly impact i-process abundance predictions, such as ^{66}Ni (55 h), ^{72}Zn (47 h), ^{135}I (6.6 h), ^{153}Sm (46 h), ^{217}Bi (98.5 s), all featuring very short half-lives, which makes them inaccessible for (n,γ) measurements via direct methods. Other relevant cases related to i-process tracers such as ^{137}Cs (30 y), ^{144}Ce (285 d) [35] may become feasible sooner. In this context, future high-flux neutron sources and innovative experimental methods, may make possible to address the direct neutron capture measurements of such reactions for the first time, as discussed in Sec. 6.

4. Highlights of stellar neutron capture measurements at CERN n_TOF

4.1. Neutron capture measurements at the n_TOF Facility

The n_TOF facility at CERN generates its neutron beams through spallation reactions of 20 GeV/c protons extracted in pulses from the CERN Proton Synchrotron and impinging onto a lead spallation target. The resulting high energy (MeV-GeV) spallation neutrons are partially moderated in a surrounding water layer to produce a white-spectrum neutron beam that expands in energy from thermal to a few GeV. The neutrons travel along two beam lines towards two experimental areas: EAR1 at 185 m (horizontal) [15] and EAR2 at 19 m (vertical) [16,36]. A new experimental area, so-called NEAR Station, has been installed during the latest upgrade next to the spallation target, as it is discussed in Sec. 5. It features an extremely high neutron flux that opens the door to (n,γ) activation measurements on short-lived radioactive isotopes or on very small mass samples [28].

In neutron TOF capture measurements at n_TOF the sample of the isotope of interest is placed in the pulsed neutron beam and the prompt capture γ -rays originating from the sample are registered by means of radiation detectors. Two different detection systems have been used for (n,γ) measurements at n_TOF so far: the 4π Total Absorption Calorimeter (TAC) [37]—a segmented detector array consisting of 40 BaF₂ crystals—and low-efficiency C₆D₆ liquid scintillators [38] in conjunction with the pulse-height weighting technique (PHWT) [39,40], which allows one to virtually mimic an ideal total energy detector (TED) [41]. The latter have been used for measurements of stellar MACS due to their reduced neutron sensitivity and fast response. Thus, all the measurements presented in this work rely on the TED principle.

Since 2001, more than 60 neutron capture cross section measurements have been carried out at the first experimental area n_TOF EAR1 [15]. Thanks to its long flight path of 185 m, EAR1 has been a reference facility for high resolution measurements on stable isotopes and samples with sufficient masses (≥ 100 mg) both in the resonance region (RRR) [42,43] and Unresolved Resonance Region (URR) up to 1 MeV [44–47], covering the full energy range of importance for astrophysics experiments. In 2014, the n_TOF Collaboration built the vertical beam line n_TOF-EAR2 [16,36], featuring a flight path of only 20 m, which delivers a substantially higher neutron flux and is particularly advantageous for measurements on radioactive samples.

4.2. Stable nuclei: s-process bottlenecks and s-only isotopes

A large fraction of the neutron-capture program at CERN n_TOF over the past 25 years has focused on nuclear astrophysics [8,9,48], addressing several of the key stable isotopes mentioned in Sec. 3, namely s-process bottleneck and s-only isotopes, and contributing to solve discrepancies between SiC grain data and model predictions.

Among other measurements, the capture cross-section of the s-only ¹⁵⁴Gd provides a direct probe of stellar neutron exposures and the efficiency of neutron sources in AGB stars, particularly the structure and extent of the ¹³C pocket, which governs the main neutron production through the ¹³C(α,n)¹⁶O reaction. Aiming at solving the observed underproduction of ¹⁵⁴Gd relative to neighboring s-only isotopes such as ¹⁵⁰Sm, a new measurement was carried out at n_TOF EAR1 [49] using low neutron-sensitivity C₆D₆ detectors. The resulting MACS₃₀ = 880(50) mb, significantly lower than previously recommended values, leads to an increase of about 10% in the predicted stellar abundance of ¹⁵⁴Gd and improves the agreement between theoretical nucleosynthesis models and observed isotopic ratio of ¹⁵⁴Gd/¹⁵⁰Sm in the solar system.

Several recent experiments also cope with s-process bottlenecks, such as ¹⁴⁰Ce or ²⁰⁹Bi. ¹⁴⁰Ce lies in the second s-process peak (N = 82). The relatively low neutron-capture cross section of isotopes in this region, gives rise to the observed abundance peak around A \approx

140. Precise neutron-capture measurements on ^{140}Ce were required to solve the existing discrepancy of 30% found between the Ce abundance predicted with AGB models and the spectroscopic observations [50]. A new measurement of this cross section was carried out at n_TOF with a highly enriched 12.3 g (Ce-oxide) sample produced at PSI. The high-resolution measurement using the aforementioned C_6D_6 setup with low neutron sensitivity covered a large neutron-energy range up to 65 keV. The relevant MACS for nucleosynthesis in AGB stars, at $kT = 8$ keV, was found to be of 28.18(24) mb, 40% higher than expected [10]. These results yielded an even smaller prediction in the s-process abundance of Ce with respect to previous estimations.

At the termination of the s-process path, ^{209}Bi represents the heaviest stable isotope and plays a key role in determining the final abundance distribution of heavy elements produced by neutron capture. The measurement of its MACS, featuring a very low value of only 2.9(5) mb at $kT = 25$ keV, together with the cross sections of the neighboring Pb isotopes (see e.g. [51]), govern the s-process termination. In particular, rather accurate abundance constraints could be derived for the r-process contribution to ^{209}Bi . With this motivation, a first neutron-capture TOF measurement on ^{209}Bi was carried out at EAR1 in 2001 [52]. However, it encountered many difficulties due to the in-beam γ -ray background and limited statistics. To overcome these limitations, a new measurement was successfully carried out in 2024 at n_TOF EAR2 [53]. The high-flux at EAR2 allowed to improve the covered energy range and the statistical accuracy with the same sample used in EAR1. Beyond this, it made possible the measurement of a new thinner (1 mm) sample for a better assessment of multiple-scattering and neutron-sensitivity effects. Moreover, the total cross section has been measured by means of transmission at JRC-Geel [54], thereby allowing a fully consistent R-matrix analysis of the two data sets.

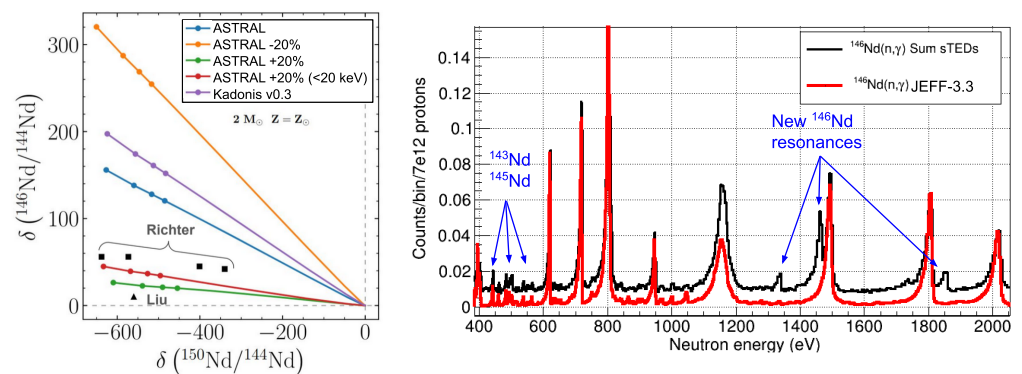


Figure 3. Left: δ -values (per mil deviations from solar system ratios) of $^{146}\text{Nd}/^{144}\text{Nd}$ relative to $^{150}\text{Nd}/^{144}\text{Nd}$ from AGB star calculations (solid lines) compared with SiC grain data (black dots) from Richter [55] and Liu [56]), showing the impact of varying the $^{146}\text{Nd}(n,\gamma)$ rate of ASTRAL [57] in $\pm 20\%$ in the full energy range and only below $kT=20$ keV. Right: Example of the counting rate measured at n_TOF EAR2 in a small range of neutron energies compared to the expected results based on JEFF-3.3.

Beyond s-only and bottleneck isotopes, an active program at n_TOF is also addressing present discrepancies between isotopic abundances measured in presolar SiC grains and the predictions of state-of-the-art s-process nucleosynthesis models. One of the recent cases is ^{146}Nd . Persistent discrepancies are observed between the predicted and measured $^{146}\text{Nd}/^{144}\text{Nd}$ ratio, which is systematically overestimated by current models, when compared to SiC data [58]. Sensitivity studies carried out with the FUNS code [59] indicate that an increase of about 15% in the ^{146}Nd neutron-capture cross section only at low stellar temperatures (below $kT=20$ keV), would significantly improve the agreement with the grain data (see Fig. 3). The available experimental information is largely based on activation

and time-of-flight data covering only the region above 3 keV [60], so-called unresolved resonance region (URR). In contrast, the capture cross section at lower energies in the so-called resolved resonance region (RRR), which strongly impacts the MACS at low stellar temperatures ($kT \approx 8$ keV), has never been measured. To address this issue, a high-resolution TOF experiment was performed at n_TOF EAR2 using a 212 mg ^{146}Nd oxide sample enriched to 97.4%, aiming at measuring both the RRR up to 5 keV and the URR up to 100 keV [61]. The TOF measurement at EAR2, for which preliminary results are shown in Fig. 3, has been complemented with an activation experiment at HiSPANoS-CNA to determine the MACS at $kT = 25$ keV. Last, this measurement has become the first case at n_TOF exploiting the complementarity between a TOF measurement and activation measurements in the new high-flux n_TOF-NEAR facility [62], thereby establishing a benchmark for future experiments made with this combination of both approaches.

4.3. Unstable nuclei: s-process branching points

Experimental efforts at CERN n_TOF have also focused on the more challenging measurement of unstable nuclei which act as branchings of the s-process. The limited sample mass available and the high background induced by the sample activity represent the major challenges to experimentally access the (n,γ) cross sections of these isotopes. To cope with such demanding requisites, a big effort has been carried out to improve the neutron beam — enhanced luminosity and improved resolution — and to reduce the γ - and neutron-induced backgrounds [8,30,63]. In parallel, the collaboration has developed an active R&D program on innovative detection systems [64–68], leading to a progressive increase in detection sensitivity for the radiative neutron-capture, that has allowed to address several first-ever TOF measurements on key s-process branchings. The reader is referred to Ref. [8] for an extended discussion on the evolution of the difficulty level of the measurements on unstable nuclei.

The early TOF measurements on unstable nuclei took place in n_TOF EAR1 between 2000 and 2015. In particular, the capture cross sections of ^{151}Sm [69], ^{93}Zr [70], ^{63}Ni [71], ^{171}Tm [23], ^{204}Tl [72] were measured. Despite the major progress related to the neutron beams and improvement in the detection sensitivity along the years, these experiments in EAR1 showed some limitations. In particular, the ^{93}Zr [70] and ^{63}Ni [71] measurements suffered from a low signal-to-background ratio (SBR) due to the neutron-induced background, which limited the neutron energy range that could be measured to few keV. More recently, the first ever TOF measurements of ^{171}Tm [23] and ^{204}Tl [72] were carried out with samples containing only few mg ($\approx 10^{19}$ atoms) produced in collaboration between ILL and PSI. The astrophysical impact of these experiments was limited by the very intense background arising from the sample activity, which restricted the upper energy for the analysis of resonances to 4 keV for ^{204}Tl and only 700 eV for ^{171}Tm . The latter is one of the relatively few cases where the TOF measurement could be complemented with an activation experiment at LiLiT-SARAF which, in turn, became crucial for improving the experimental uncertainty of MACS_{30} to about 10%. In practice, the idea of complementing TOF and activation was among the motivations to build the n_TOF-NEAR station, discussed in Sec. 5 and the project for the future n_ACT (see Sec. 6).

A major upgrade to address the challenging background arising from radioactive samples was the deployment of EAR2. Thanks to its ≈ 10 -times shorter flightpath compared to EAR1, it features a 400-times higher instantaneous neutron flux (see Ref. [73]). This beamline is particularly well suited for neutron-capture measurements on highly radioactive and/or very small mass samples, such as s-process branching nuclei. Later, in 2021, the n_TOF facility installed its third generation spallation target [74] during the CERN Long Shutdown 2 (LS2) (2019–2021). The optimized design of this new spallation target

brought a remarkable upgrade of the performance of EAR2, both on the energy resolution and the neutron flux [63]. Details on the upgraded facility performance can be found in Ref. [75,76].

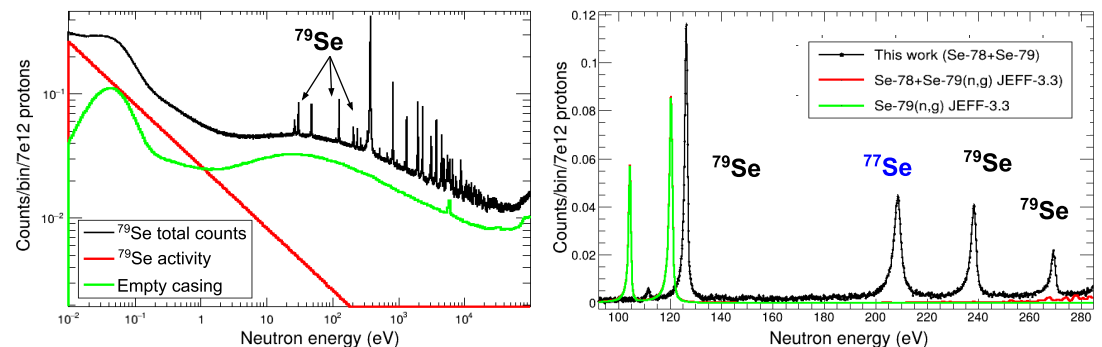


Figure 4. Left: Total counts and background components as a function of the neutron energy measured with the PbSe ($^{78}\text{Se}+^{79}\text{Se}$) sample in n_TOF EAR2. The first resonances of ^{79}Se are highlighted. Right: Background-subtracted $^{79}\text{Se}(n,\gamma)$ yield showing examples of observed resonances compared to the expected results based on JEFF-3.3.

Improving the characteristics of the neutron beam is not sufficient to overcome all the existing challenges for (n,γ) measurements on several unstable branching points. To this end, together with the unprecedentedly high luminosity of EAR2 target, a new generation of C_6D_6 detectors with higher segmentation, so-called sTED [67], have been developed to cope with the high count rates associated to the flux of EAR2 [77]. The arrangement of the 9 sTED cells in a compact-ring configuration around the capture sample has enhanced the sensitivity [77,78]. In addition, for those cases where the neutron-induced background dominates [70,71], an innovative solution based on Total-Energy Detection (TED) with γ -ray imaging capability, so-called i-TED, was proposed [65]. i-TED exploits the Compton imaging technique with the aim of determining the direction of the incoming γ -rays. This allows the rejection of events not originating in the sample, thereby enhancing the signal-to-background ratio (SBR). i-TED has been developed [79–81] and successfully validated at n_TOF [66,82] in recent years.

The recent upgrades on detection systems and spallation target have allowed to reach an unprecedented sensitivity (see Fig. 2 of Ref. [8]), as it is demonstrated by the first-ever capture measurements on the unstable ^{94}Nb (half-life, $T_{1/2} = 2.3 \times 10^4$ y) [78,83] and ^{79}Se ($T_{1/2} = 3.27 \times 10^5$ y) [77] isotopes. Focusing on the latter, the branching at ^{79}Se is particularly well suited for determining the thermal conditions of the stellar environment thanks to the strong thermal dependence of its beta decay rate [3]. For this experiment, 2.7 mg of ^{79}Se were produced by means of neutron irradiation of an enriched $^{208}\text{Pb}^{78}\text{Se}$ alloy-sample in the high-flux reactor at ILL [77,84]. This measurement combined EAR1 using i-TED and EAR2 using the sTED array [77]. The data analysis has shown the relevance of having a high instantaneous flux of EAR2 to cope with the background arising from unavoidable activation in the sample (5 MBq and 1.4 MBq for ^{75}Se and ^{60}Co , respectively), see Fig. 4. The quality of the TOF data has allowed analyzing for the first time 12–13 resonances up to ≈ 1.25 keV. So far, there are only theoretical predictions of the cross section, as those adopted in JEFF-3.3. However, this prediction can never be reliable as illustrated in Fig. 4. The final analysis will provide the first experimental value for the MACS, leading to a constraint of the thermal conditions of the weak s-process in massive stars.

5. Current limits and recent advances

5.1. Pushing the limits for TOF measurements in EAR2

Neutron capture measurements on unstable isotopes have been already successfully measured at n_TOF using samples with masses $\simeq 1\text{--}50$ mg [23,77,78,85,86]. Measurements of lower masses are still difficult, for instance a $^{147}\text{Pm}(n,\gamma)$ measurement at EAR2 on a sample of only $85\ \mu\text{g}$, allowed to see only the 3 first resonances due to the limited SBR [31,87].

The recent improvements in the performance of the n_TOF neutron beams and detection systems has led to an improved sensitivity in (n,γ) measurements. In this context, a systematic study of the current detection limit in the upgraded n_TOF EAR2 has been carried out [88] for TOF measurements on key s-process branching isotopes listed in Refs. [3,17]. Among the challenging key s-process points never measured before via TOF [3,17], we have selected ^{81}Kr , ^{135}Cs , ^{147}Pm , ^{153}Gd , ^{163}Ho , ^{179}Ta , which present sufficiently long half-lives to prepare a target ($\simeq 1$ y) combined with the emission of no γ -rays or only low-energy γ -rays which could be efficiently shielded. The list of studied isotopes, their main properties, challenges for the TOF measurement and complementarity with activation are summarized in Table 2.

Table 2. Summary of s-process branching points included in the feasibility study for TOF (n,γ) measurement in the upgraded n_TOF EAR2 [88].

Isotope	$T_{1/2}$	A (1×10^{17} at)	Decay	Activation ($T_{1/2}$ product)
^{81}Kr	2.29×10^5 y	9.60 kBq	γ : 275 keV, EC	No
^{135}Cs	2.30×10^6 y	956 Bq	No γ , $Q_{\beta}=286$ keV	Yes (13 d)
^{147}Pm	2.62 y	839 MBq	No γ , $Q_{\beta}=224$ keV	Yes (5.4 d)
^{153}Gd	240 d	3.4 GBq	γ : <100 keV, EC	No
^{155}Eu	4.68 y	470 MBq	γ : 86,105 keV, $Q_{\beta}=252$ keV	Yes (15.19 d)
^{163}Ho	4.57×10^3 y	481 kBq	No γ , EC	Yes (30 min)
^{179}Ta	1.82 y	1.21 GBq	No γ , EC	Yes (8 h)

To study the feasibility of such experiments with the current sensitivity of EAR2, we have carried out simulations of the anticipated experimental outcomes for different sample masses ranging from 5×10^{16} atoms up to 5×10^{18} atoms. To realistically predict the statistical uncertainties we have implemented a Monte Carlo (MC) resampling method and assigned a realistic number of protons to the sample (corresponding to 30 days of measurement) and the background characterization (20 days) measurements. The isotopes of this study do not present high energy γ -ray activity and, thus, the major background source is expected to be the neutron-beam related background similarly to the situation of the recent ^{94}Nb and ^{79}Se measurements. Fig. 5 shows the expected capture yield for the potential $^{155}\text{Eu}(n,\gamma)$ and $^{179}\text{Ta}(n,\gamma)$ with samples of, respectively 5×10^{17} and 1×10^{18} atoms. Here individual resonance parameters were taken from JEFF-3.3 and have been randomly generated based on average resonance parameters.

Based on the simulated experiments, we have quantified the expected number of observable resonances and the maximum neutron-energy range accessible for their identification. For each resonance, the probability of observation was evaluated using a statistical detection criterion following the methodology adopted in recent experiment preparation studies [89]. The results, shown in Fig. 6 for the two representative isotopes, indicate that with the current signal-to-background ratio at n_TOF-EAR2, samples containing

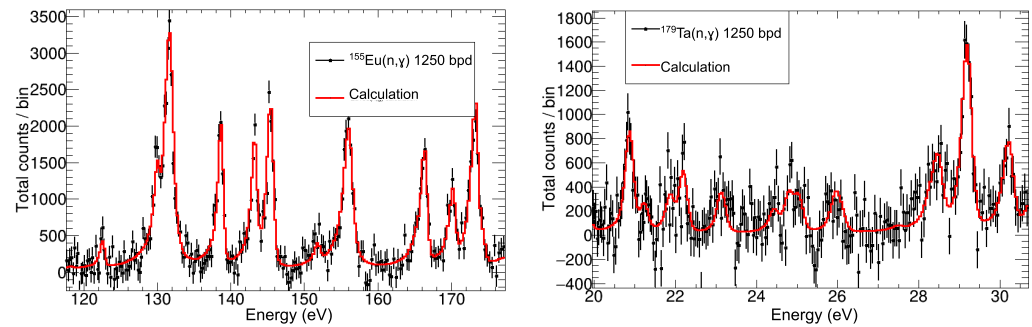


Figure 5. Expected capture yield with 1250 bins per decade (bpd) after the background subtraction compared to the expected yield based on the simulated resonance parameters for a ^{155}Eu sample of 5×10^{17} atoms (left) and a ^{179}Ta sample of 10^{18} atoms.

1×10^{17} – 5×10^{18} atoms (depending on the isotope), corresponding to sample masses of about 30–1500 μg , would be required to observe a sufficient number of resonances to allow a reliable determination of the average resonance parameters needed for the extrapolation of the MACS. In practice, at least 10–15 observed resonances are required for this purpose [23,72,83]. Nonetheless, such sample masses are often beyond currently attainable quantities or cannot be produced with sufficient isotopic purity, highlighting the need for improved radiochemical production methods [90]. The study also indicates that the signal-to-background ratio achievable in these TOF measurements would not allow a direct determination of the cross section in the unresolved resonance region (URR), which represents a large fraction of the neutron-energy range of astrophysical interest. For several of the studied isotopes — ^{135}Cs , ^{147}Pm , ^{155}Eu , ^{163}Ho , and ^{179}Ta — a complementary activation measurement could therefore be envisaged (see Table 2). Activation measurements will now be possible at CERN after the deployment of the n_TOF-NEAR station and the proposal of the future n_ACT activation facility discussed in the following.

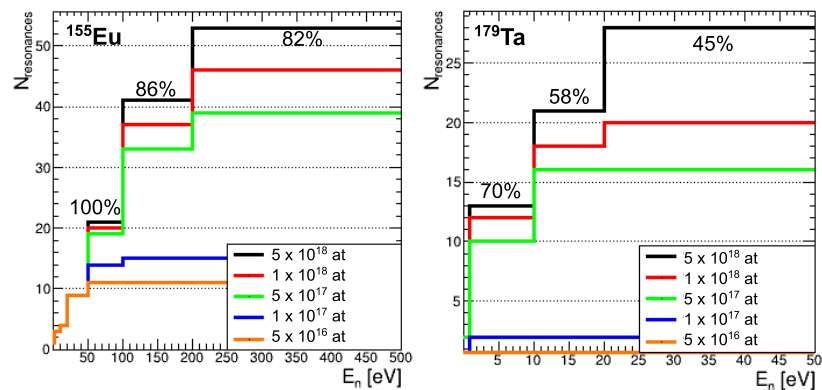


Figure 6. Expected number of cumulative observed s-wave resonances in different neutron energy ranges for ^{155}Eu and ^{179}Ta (4σ detection threshold). The cumulative fraction of observed resonances at the end of the energy range is provided (only for the thickest sample). Samples of 10 mm diameter and different masses are compared.

As discussed along this section, direct capture measurements in the full energy range of stellar interest via TOF still require further optimization of the sensitivity. In particular, an improved SBR to access smaller sample mass ($\leq 100 \mu\text{g}$), would be required. Starting from the state-of-the-art (n,γ) setup based on sTED detectors in a compact ring configuration [77], the n_TOF collaboration has launched a series of optimization campaigns of the signal-to-background ratio (SBR) at EAR2 [91,92]. The efforts split in two directions: maximizing the detected (n,γ) events and reducing the beam-induced background.

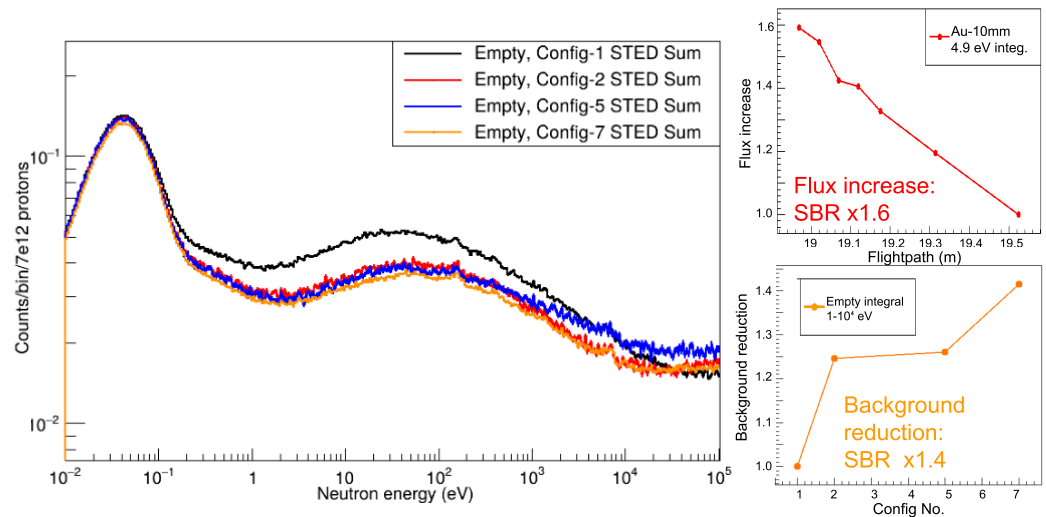


Figure 7. Left: *Empty* background in n_TOF EAR2 measured with the array of 9 STED detector. The reference level (black) is compared with improved shielding configurations that provided an absolute reduction of the background. Left: Summary of the signal-to-background (SBR) gain obtained due to an increase in the flux intercepted by the sample (top) and due to the reduction of the empty sample background (bottom).

The signal can be enhanced, by increasing the fraction of the neutron beam impinging on the sample, the so-called Beam Interception Factor (BIF). Recent results, shown in Fig. 7, demonstrate that as a consequence of the spatial divergence of the beam in EAR2 [16], the BIF can be enhanced by shortening the flight-path (L) in the experimental hall of EAR2. An improvement in the SBR by a factor of 1.6 was found for 10 mm diameter samples when bringing the sample and detectors 60 cm closer to the second collimator without any negative impact on the background. The (n, γ) sensitivity can be further enhanced by increasing the efficiency for detecting γ -rays emitted from the sample. This objective has motivated further R&D efforts toward larger segmented arrays of C_6D_6 detectors [93] or novel compact solid scintillators with higher intrinsic efficiency [68].

The remaining critical aspect for further improving the SBR is the reduction of the beam-induced background unrelated to the sample, so-called *Empty* background in Fig. 7. This background is intrinsic to the facility and depends largely on the effectiveness of the shielding against the uncollimated neutrons. The facility's unique combination of a short flight path and presence of high energy neutrons up to 350 MeV complicates the design of a collimation system focused on the reduction of the background in (n, γ) experiments. The results of the recent optimization campaigns showed that, by improving the neutron shielding after the second collimator, the background could be reduced by a factor of 1.45 (see Fig. 7). The combined increase in the (n, γ) signal and reduction of the background thus resulted in a 2.5-fold improvement in the SBR. These promising results have motivated a more detailed design study of a new shielding system aimed at achieving further substantial gains in sensitivity after LS3 (2026–2028).

5.2. The n_TOF-NEAR: a high flux activation facility

As it was introduced in Sec. 2, the activation technique shows an unsurpassed sensitivity and represents an advantage for the measurement of very small sample masses, where the limited signal-to-background ratio would represent an important limitation for the TOF measurement. In practice, combining neutron TOF and activation measurement, when feasible, may deliver complementary and more accurate information on a specific cross section, see e.g. [23,87].

As already mentioned above, following these premises, the n_TOF facility expanded in 2021 its experimental capabilities with the deployment of the NEAR station [28]. Located at a distance of only 2.5 m from the lead spallation target, it features 2 orders of magnitude higher neutron flux than EAR2. The high flux makes it well suited for activation measurements on extremely small mass samples ($\leq 1\mu\text{g}$) and on radioactive isotopes which, as discussed in Sec. 5, are often not feasible via TOF. Conceptual MC simulations [8,28] showed the possibility of using moderating materials (e.g. Al-oxide, Be) followed by B_4C filters for producing quasi-Maxwellian neutron-energy spectra over a broad range of temperatures between about 1 and 100 keV, making this facility unique when compared with stellar neutron beams at $kT = 25$ keV. After a few years of development and commissioning [94], the energy-tuning setup is now fully implemented after the recent installation of a 20 cm thick Al-oxide moderator [95] which smoothens the flux and suppresses the undesired MeV-neutrons component [8]. The activated samples are then measured at the Gamma-ray spectroscopy Experimental Area (GEAR) of n_TOF, which is at the moment based on a CANBERRA HPGe detector GR5522 (63% efficiency) supplemented with a low-background shielding [28].

Besides the possibility to exploit the complementarity between TOF and activation, illustrated with the recent ^{146}Nd measurement (see Sec. 4), NEAR aims at pushing the limits for the direct capture measurements on radioactive nuclei not accessible by TOF. The first unstable isotope of astrophysical interest proposed for an activation MACS measurement at NEAR is ^{135}Cs ($T_{1/2} = 2$ Myr) [96]. The stellar neutron-capture rate of ^{135}Cs is of particular relevance as a part of the temperature-dependent s-process branching at $A = 134\text{--}135$ [97], which fixes the branching ratio between the two s-only ^{136}Ba and ^{134}Ba , well characterized from SiC in presolar grains [98]. The neutron capture of ^{135}Cs at $kT = 25$ keV was already measured at FZK [99] and therefore this measurement could be a good benchmark case for the performance of the new facility. In addition, at NEAR the MACS could also be completed for lower neutron energy ranges around $kT = 8$ keV, where presently there is no experimental information available.

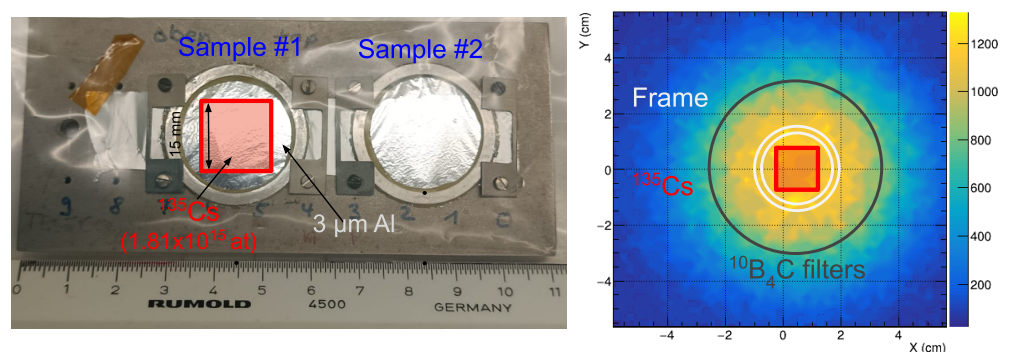


Figure 8. Left: Sample backing where ^{135}Cs was implanted on the holder of the ISOLDE SSP chamber. Right: Sketch of the sample inserted in the filters overlaid with the neutron beam profile at NEAR. The color scale represents the neutron flux in a.u.

A suitable sample of ^{135}Cs of 1.81×10^{15} atoms, sketched in Fig. 8, has been ion-implanted on a $3\mu\text{m}$ thick aluminum backing in the Solid State Physics (SSP) chamber of ISOLDE [100]. The ^{135}Cs beam was produced and mass-separated using the General Purpose Separator using as an ion source a commercial ^{137}Cs liquid source of 9 MBq featuring an isotopic ratio $^{135}\text{Cs}/^{137}\text{Cs}=0.72$. The sample backings were designed to fit in the B_4C discs used for the aforementioned energy filtering at NEAR, where the beam dimensions are much larger than the $15 \times 15\text{mm}^2$ implanted area (see Fig. 8). After the irradiation, the decay of the activation product, ^{136}Cs ($T_{1/2} = 13$ d), could be measured

at the GEAR station or in other high-efficiency HPGe-based setups (available at CERN). This experiment would show the potential synergy to perform activation measurements at NEAR on small samples of highly isotopically enriched samples produced in the nearby ISOLDE facility.

6. New ideas and future projects

While the recent upgrades at n_TOF have substantially improved present capabilities, fully addressing the remaining challenges requires the development of novel experimental concepts and facilities. This section outlines complementary experimental concepts that aim to overcome the limitations identified in Sec. 5 by either increasing neutron flux, extending energy coverage, or developing new methods to access short-lived nuclei.

6.1. New high-flux activation facilities at CERN

6.1.1. The n_TOF-NEAR facility with CYCLING

To date, activation measurements at NEAR consist of week-long irradiations followed by manual retrieval and transport to the GEAR. In this single-activation scheme, the time required to cool-down the NEAR bunker after the end of the irradiation (6 h) and transport the sample to the offline detector, imposes an intrinsic limit on the minimum half-life of the (n,γ) product. This limitation could be overcome with the installation of a CYCLIC activation station for (N,G) experiments (CYCLING) at NEAR [88,101], the repetition of a short irradiation, rapid transfer to a detector located nearby, measurement of the decay and transport back to the irradiation position [102]. Such a remote sample transport system at NEAR would also allow the remote retrieval of any irradiated samples, thereby reducing the duration and frequency of beam stops to access NEAR.

Depending on the duration of the transport of the sample to the detector, half-lives of the order of seconds or minutes would become accessible. There are several isotopes of great interest for stellar nucleosynthesis studies that could be investigated with the proposed CYCLING station. Some of them are stable nuclei, such as ^{19}F , which leads to the formation of ^{20}F ($T_{1/2} = 11$ s) [101]. Among the s-process branching nuclei listed in Table 2, the activation measurements of $^{163}\text{Ho}(n,\gamma)^{164}\text{Ho}$ ($T_{1/2} = 30$ min) and $^{179}\text{Ta}(n,\gamma)^{180}\text{Ta}$ ($T_{1/2} = 8$ h) would also benefit of a cyclic scheme at NEAR. In addition to s-process cases, (n,γ) measurements on isotopes of relevance for the intermediate (*i*-) neutron capture process [5], such as $^{137}\text{Cs}(n,\gamma)^{138}\text{Cs}$ ($T_{1/2} = 33$ min) or $^{144}\text{Ce}(n,\gamma)^{145}\text{Ce}$ ($T_{1/2} = 2.8$ min) [30,88], could be accessible for the first time with CYCLING.

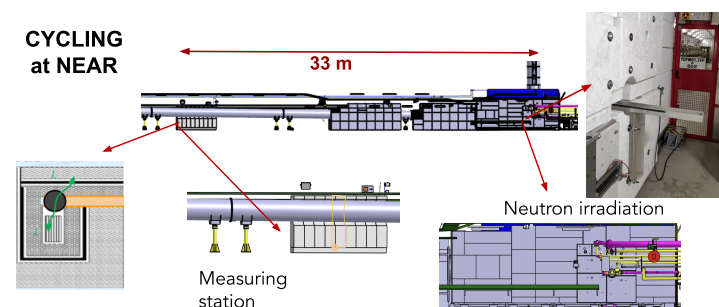


Figure 9. Sketch of the CYCLING project showing the irradiation point for activations at NEAR (a-NEAR) and the measuring station, proposed to be at 33 m in the tunnel towards EAR1, that would be connected by a remote transport system.

The feasibility of this station depends mainly on the capability to operate active detectors in the harsh radiation environment near the NEAR bunker and thus the design of the measuring station requires a good knowledge of the expected neutron and γ -ray

fields. With this goal, several campaigns have been carried out to assess the mixed neutron-gamma radiation field at several positions in the NEAR and validate the first simulation results [88]. The sensitivity to measure the decay of activated samples has been explored using a portable decay station consisting on a cylindrical 1.5'' \times 1.5'' LaBr₃(Ce) Canberra detector with shielding for neutrons (borated polyethylene) and γ -rays (steel) that has been placed in various positions around the NEAR facility. Based on these campaigns, the preferred location, which provides a sufficiently low background, is 33 meters away from the irradiation point in the downstream tunnel towards EAR1 and shielded from the neutrons a large concrete shielding, see Fig. 9.

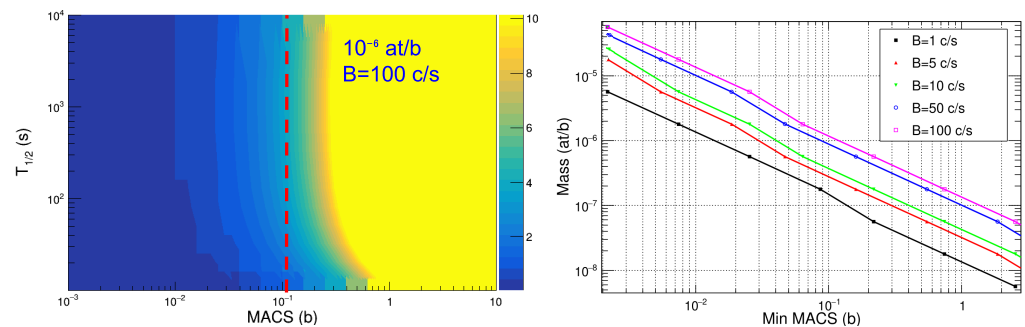


Figure 10. Left: Simulated statistical significance (colour scale in σ) for the detection of decay a γ -ray in a cyclic activation scheme as a function of the MACS₃₀ and the half-life of the (n,γ) product nucleus. These results correspond to the scenario for the background of $\simeq 100$ c/s in a HPGe. The red dashed line indicates the minimum MACS measurable (at the significance level of 4σ). Right: Mass required as a function of the minimum detectable MACS₃₀ (Min MACS) for different background levels in the final measuring station with an optimized shielding.

Based on the signal-to-background ratio achieved in the experimental campaign, a systematic study of cases that would be measurable in CYCLING has been carried out. A numerical simulation of a cyclic activation scheme was performed assuming a fixed transport time of 15 s, irradiation and counting times of $1.5 \times T_{1/2}$ and a time-averaged neutron flux of 3.07×10^7 n/s, corresponding to the energy-filtered flux integrated over a sample of 10 mm radius. The feasibility has been studied as a function of the (n,γ) product $T_{1/2}$, the MACS₃₀ and the areal density of the activated sample. From the results, we have evaluated the statistical significance for observation of a photo-peak corresponding to the γ -ray decay of the product nucleus. Fig. 10 shows the results for this baseline scenario – based on the background level found in the exploratory campaigns of ≈ 100 c/s below the 412 keV photo-peak of the ¹⁹⁸Au decay. The results show that the $T_{1/2}$ of the (n,γ) product does not impact the feasibility, except for cases where it is comparable to the transport time. The study concluded that the assumed background level would allow one to measure MACS₃₀ in the range of 10–1000 mb with samples of 10^{-7} – 10^{-5} at/b, corresponding to 10^{17} – 10^{19} atoms (see right panel of Fig. 10). The final attainable sensitivity would depend on the level of background after an optimized design of the built measuring station.

For unstable isotopes, the background will in most cases be dominated by the intrinsic activity of the sample itself, and the feasibility of such experiments will depend strongly on the decay-energy spectrum and the detector counting-rate capabilities, thus requiring a case-by-case optimization of the setup. Among the most challenging cases discussed above is ¹³⁷Cs: a sample of $\sim 1 \times 10^{17}$ atoms would correspond to an activity of about 70 MBq dominated by the 662 keV γ -ray line. In this scenario, a viable strategy could rely on high count-rate detectors such as LaBr₃(Ce), combined with a relatively high energy threshold or the use of a lead absorber to suppress the intense 662 keV radiation, thereby enabling the detection of the higher-energy (≥ 1 MeV) γ rays from the decay of ¹³⁸Cs.

The implementation of CYCLING would require the installation of a remote transport system that is able to cover the 30 m distance in tens of seconds. The design phase of the project has been launched and, if a viable solution is found, it could be developed and installed at CERN before the end of LS3.

6.1.2. The n_ACT at BDF facility

To expand further on the large potential of the activation technique and on its complementarity with TOF experiments, the n_ACT facility at the SPS Beam Dump Facility (BDF) has been proposed at CERN [29]. n_ACT will be a high-flux neutron activation station integrated into the BDF target, which can be operated parasitically to the Search for Hidden Particles (SHiP) experiment. The high intensity neutron fields produced by spallation reactions of the 400 GeV/c, 4×10^{13} p/pulse proton beam from the SPS accelerator in the tungsten target, can be exploited for accurate neutron activation measurements.

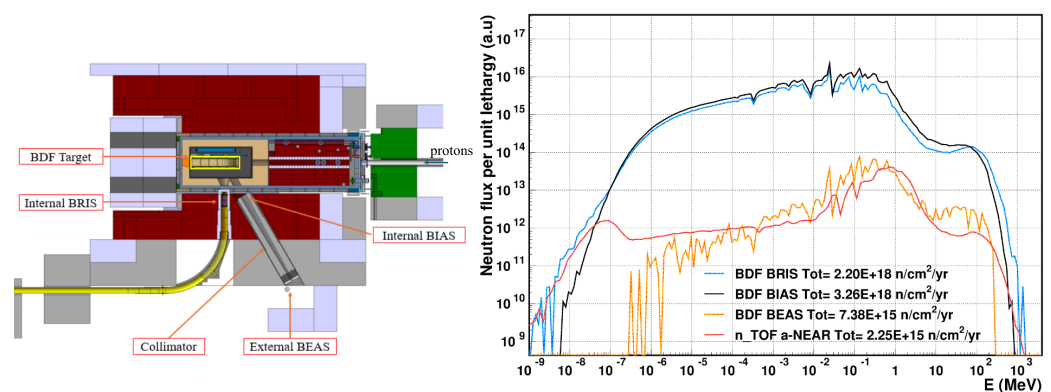


Figure 11. Left: Layout of the proposed n_ACT Activation Stations and the main components of the BDF target station. Right: Neutron spectra at BDF irradiation stations (BRIS, BIAS and BEAS) compared with n_TOF a-NEAR. Figure taken from Ref. [29].

n_ACT will comprise three complementary activation stations integrated into the BDF target complex (see Fig. 11) offering ultra-high-flux close-target neutron fields for long-term irradiations (BIAS), a rabbit system to connect with an external radiochemistry and spectroscopy lab (BRIS), and a collimated external neutron beam (BEAS), thereby covering the full range of activation needs. As shown in Fig. 11, BIAS and BRIS would provide neutron fluxes up to three orders of magnitude higher than that of a-NEAR. n_ACT would profit from the filtering method developed at NEAR to tailor the neutron spectra to different stellar kT values (2–60 keV). Being at CERN, this facility would profit from the unique complementarity with n_TOF — energy-resolved via TOF combined with high-flux activation — and proximity to ISOLDE for producing short-lived isotopes and should enable the world-first measurements on several rare and unstable nuclei.

6.2. TOF-DONES: A time-of-flight facility at IFMIF-DONES

As discussed in Sec. 5, pushing the limits of TOF capture measurements requires developing new facilities that can substantially improve the performance of the existing ones. With this aim, a TOF facility at the IFMIF-DONES facility, is being designed [103]. At TOF-DONES, the extraction of 0.1% of the 40-MeV deuteron beam bunched in 5.3 ns pulses with a maximum repetition rate of 175 kHz, would be used for driving one of the most intense neutron TOF facilities. The performance in terms of time-averaged neutron flux of two TOF-DONES beam lines when compared with existing leading neutron TOF facilities is shown in figure 12.

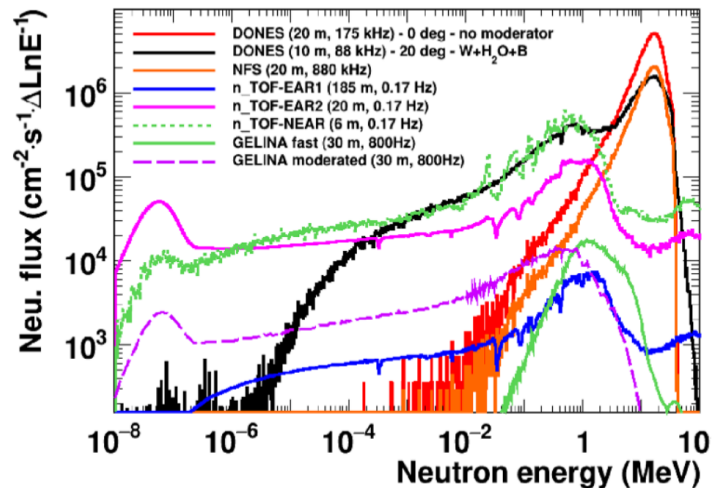


Figure 12. Average neutron flux at different TOF beamlines in TOF-DONES compared to other existing TOF facilities. Figure taken from Ref. [103].

The TOF-DONES facility is projected to have a graphite neutron production target and several flight paths with different moderation, that would provide similar or even higher neutron flux of the currently most intense TOF facilities above 10 keV (see Fig. 12). The unmoderated neutron spectrum would enable to have a world-leading intensity of fast neutrons, higher than that of the NFS facility at GANIL. In addition, one of the foreseen beamlines would have a moderated spectrum that would extend the neutron energies down to the astrophysical range of interest with an average flux larger than that of n_TOF EAR2.

6.3. Inverse kinematics with storage rings and neutron targets

Direct capture measurements using neutron beams and targets of the isotope of interest will never allow accessing short-lived nuclei ($T_{1/2} \leq$ days) of relevance for the s-, i- and r-process. To tackle these cases, a promising approach for the long-term future consists of performing direct neutron-capture reactions in inverse kinematics by circulating radioactive ions in a storage ring intersecting a localized free-neutron target [104,105]. In this concept, ions repeatedly traverse a confined neutron field, dramatically enhancing the effective luminosity and enabling direct measurements on short-lived nuclei that cannot be prepared as conventional samples. With the inverse kinematics method, direct measurements of neutron-capture cross sections at different stellar temperatures could be performed by changing the ion-beam energy.

The first conceptual realization of this idea was based on the use of a nuclear reactor [104]. A more feasible approach was proposed later based on a spallation neutron source [105]. In the latter high-energy protons impinge on a tungsten target surrounded by a heavy-water moderator, producing a high intensity, moderated neutron field overlapping the ion beam pipe of a storage ring. In parallel, a new initiative focuses on developing a compact cyclotron-driven neutron target, where neutrons are produced via low-energy ${}^9\text{Be}(p,xn)$ reactions and subsequently moderated and confined around the storage-ring beam pipe using optimized moderator and reflector assembly [106]. This design enables a fully integrated and scalable neutron target system aimed at compatibility with existing or future storage rings. Building on this concept, several facilities are actively developing projects in this direction. At TRIUMF-ISAC, the proposed TRISR storage ring aims at integrating a compact neutron source directly within the ring lattice, enabling circulating radioactive ions from the ISOL facility to interact with moderated neutrons [4]. Another

neutron target project aims to validate the concept at CRYRING@ESR (GSI) (see Fig. 10 of Ref. [106] for the proposed implementation). The overall performance would then be further boosted by several orders of magnitude [106] by integrating this neutron target in specially designed ion storage such as TRISR at TRIUMF [4] or ISR at ISOLDE [107].

Examples for neutron capture measurements of astrophysical interest that could become accessible for a direct measurement with this concept are some of the s-process branching points which remain unmeasured, e.g. ^{147}Nd ($T_{1/2} = 11$ d), ^{148}Pm ($T_{1/2} = 5.4$ d), ^{160}Tb ($T_{1/2} = 72$ d) and ^{170}Tm ($T_{1/2} = 128$ d) as well as shorter-lived isotopes with high impact in the i-process abundances, such as ^{66}Ni ($T_{1/2} = 55$ h), ^{72}Zn ($T_{1/2} = 47$ h), ^{135}I ($T_{1/2} = 6.6$ h), ^{141}Ba ($T_{1/2} = 18$ min), ^{141}La ($T_{1/2} = 3.9$ h) and ^{153}Sm ($T_{1/2} = 46$ h).

7. Summary and outlook

Neutron-capture reactions remain one of the fundamental nuclear-physics inputs governing the synthesis of heavy elements in stars. Despite more than five decades of experimental effort, significant challenges persist in achieving the level of accuracy and completeness now demanded by modern astrophysical observations. High-precision isotopic measurements from presolar SiC grains, improved spectroscopic stellar abundances, and increasingly sophisticated stellar models require neutron-capture cross sections with uncertainties at or below the 5% level over the full stellar energy range. In addition, key branching-point isotopes and nuclei relevant for the intermediate (i-) process remain largely unexplored experimentally.

In this work, we have reviewed recent advances in direct neutron-capture measurements at CERN n_TOF, highlighting both achievements and present limitations. Time-of-flight (TOF) experiments at n_TOF have significantly improved the knowledge of cross sections for s-only isotopes and bottleneck nuclei, such as ^{154}Gd , ^{140}Ce and ^{209}Bi , directly impacting stellar abundance predictions. In parallel, substantial progress has been achieved in the measurement of unstable branching-point nuclei, including first-time capture measurements of isotopes such as ^{94}Nb and ^{79}Se . These results have been driven by the high luminosity of EAR2, the development of advanced detection systems such as sTED and i-TED, and continuous optimization of the signal-to-background ratio.

At the same time, systematic feasibility studies show that even with state-of-the-art TOF facilities like n_TOF EAR2, measurements of s-process branching-point isotopes remain limited by sample availability, background conditions, and restricted energy coverage. In several cases, only the resolved resonance region can be accessed with realistic sample masses, leaving the Maxwellian averaged cross sections at higher stellar temperatures insufficiently constrained. In this context, the complementarity between TOF and activation techniques emerges as a central strategy for the next generation of neutron-capture experiments. The commissioning of the high-flux n_TOF-NEAR activation station opens new possibilities for measuring extremely small or radioactive samples and for tailoring quasi-Maxwellian neutron spectra over a wide range of stellar temperatures. The case of ^{146}Nd illustrates this synergistic approach: a high-resolution TOF measurement in the resonance region, combined with activation data at different kT values, enables a consistent re-evaluation of the stellar rate and directly addresses discrepancies between s-process models and presolar grain data.

Looking ahead, further sensitivity gains are expected from future optimization of n_TOF setups during CERN LS3. The proposed CYCLING station at n_TOF NEAR would extend activation measurements to short-lived reaction products. In parallel, the n_ACT project at the CERN Beam Dump Facility and the development of TOF-DONES would provide substantially higher neutron fluxes and complementary energy coverage opening access to new s- and i-process cases. In the even longer term, inverse-kinematics approaches

using storage rings in which unstable ion beams circulate through localized neutron targets offer a novel path toward direct measurements on short-lived nuclei ($T_{1/2} \leq$ days) that are inaccessible today. Continued progress along these lines will be essential for reducing the remaining nuclear-physics uncertainties and for fully exploiting the precision of modern astrophysical observations in unraveling the origin of heavy elements.

Author Contributions: Conceptualization, J.L.M.; methodology, J.L.M.; formal analysis, J.L.M.; investigation, n_TOF-Collaboration; resources, n_TOF-Collaboration; data curation, J.L.M.; writing—original draft preparation, J.L.M.; writing—review and editing, C.D.P.; Supervision: C.D.P.; project administration: C.D.P, J.L.M.; funding acquisition: C.D.P, J.L.M.,. All authors have read and agreed to the published version of the manuscript.

Funding: This research received no external funding apart from those included in the acknowledgments section.

Data Availability Statement: The datasets generated during and/or analyzed during the current study are available from the corresponding author on reasonable request.

Acknowledgments: Part of this work was supported by the European Research Council (ERC) under the European Union’s Horizon 2020 research and innovation programme ERC-COG No. 681740 and ERC-STG No. 677497, European H2020-847552 (SANDA) and EURO-LABS (grant agreement No. 101057511). The authors acknowledge support of the Spanish MCIN/AEI 10.13039/501100011033 under grants Severo Ochoa CEX2023-001292-S, PID2022-138297NB-C21, PID2019-104714GB-C21. J.L.M acknowledges support of grant FJC2020-044688-I funded by MCIN/AEI/ 10.13039/501100011033 and European Union NextGenerationEU/PRTR, and grant CIAPOS/2022/020 funded by the Generalitat Valencia and the European Social Fund. Authors also acknowledge the funding agencies of the participating n_TOF institutions and Infrastructure Access Agreement N° 35543/1/2019-1-RD-EUFRAT-GELINA.

Conflicts of Interest: The authors declare no conflicts of interest.

References

1. Burbidge, E.M.; Burbidge, G.R.; Fowler, W.A.; Hoyle, F. Synthesis of the Elements in Stars. *Rev. Mod. Phys.* **1957**, *29*, 547–650. <https://doi.org/10.1103/RevModPhys.29.547>.
2. Cameron, A.G.W. On the origin of the heavy elements. *Astrophysical Journal* **1957**, *62*, 9–10. <https://doi.org/10.1086/107435>.
3. Käppeler, F.; Gallino, R.; Bisterzo, S.; Aoki, W. The s process: Nuclear physics, stellar models, and observations. *Reviews of Modern Physics* **2011**, *83*, 157–194, [arXiv:astro-ph.SR/1012.5218]. <https://doi.org/10.1103/RevModPhys.83.157>.
4. Dillmann, I.; Kester, O.; Baartman, R.; Chen, A.; Junginger, T.; Herwig, F.; Kaltchev, D.; Lennarz, A.; Planche, T.; Ruiz, C.; et al. Measuring neutron capture cross sections of radioactive nuclei. *The European Physical Journal A* **2023**, *59*, 105. <https://doi.org/10.1140/epja/s10050-023-01012-9>.
5. Cowan, J.J.; Rose, W.K. Production of ^{14}C and neutrons in red giants. *Astrophysical Journal* **1977**, *212*, 149–158. <https://doi.org/10.1086/155030>.
6. Hampel, M.; Stancliffe, R.J.; Lugaro, M.; Meyer, B.S. THE INTERMEDIATE NEUTRON-CAPTURE PROCESS AND CARBON-ENHANCED METAL-POOR STARS. *The Astrophysical Journal* **2016**, *831*, 171. <https://doi.org/10.3847/0004-637X/831/2/171>.
7. Pignatari, M.; Gallino, R.; Heil, M.; Wiescher, M.; Käppeler, F.; Herwig, F.; Bisterzo, S. THE WEAK S-PROCESS IN MASSIVE STARS AND ITS DEPENDENCE ON THE NEUTRON CAPTURE CROSS SECTIONS. *The Astrophysical Journal* **2010**, *710*, 1557–1577. <https://doi.org/10.1088/0004-637x/710/2/1557>.
8. Domingo-Pardo, C.; Aberle, O.; Alcaayne, V.; Alpar, G.; Halabi, M.A.; Amaducci, S.; Babiano, V.; Bacak, M.; Balibrea-Correa, J.; Bartolomé, J.; et al. Neutron capture measurements for s-process nucleosynthesis. *The European Physical Journal A* **2025**, *61*, 105. <https://doi.org/10.1140/epja/s10050-025-01563-z>.
9. Massimi, Cristian.; The n_TOF Collaboration. Nuclear astrophysics activities at the n_TOF facility at CERN. *EPJ Web Conf.* **2023**, *275*, 01009. <https://doi.org/10.1051/epjconf/202327501009>.
10. Dillmann, I.; Szücs, T.; Plag, R.; Fülöp, Z.; Käppeler, F.; Mengoni, A.; Rauscher, T. The Karlsruhe Astrophysical Database of Nucleosynthesis in Stars Project – Status and Prospects. *Nuclear Data Sheets* **2014**, *120*, 171–174. <https://doi.org/https://doi.org/10.1016/j.nds.2014.07.038>.

11. D. Ene et al.. Global characterisation of the GELINA facility for high-resolution neutron time-of-flight measurements by Monte Carlo simulations. *Nuclear Instruments and Methods in Physics Research Section A: Accelerators, Spectrometers, Detectors and Associated Equipment* **2010**, 618, 54–68. <https://doi.org/https://doi.org/10.1016/j.nima.2010.03.005>.
12. L. Zavorka et al.. Physics design of the next-generation spallation neutron target-moderator-reflector-shield assembly at LANSCE. *Nuclear Instruments and Methods in Physics Research Section A: Accelerators, Spectrometers, Detectors and Associated Equipment* **2018**, 901, 189–197. <https://doi.org/https://doi.org/10.1016/j.nima.2018.06.018>.
13. K. Kino et al.. Energy resolution of pulsed neutron beam provided by the ANNRI beamline at the J-PARC/MLF. *Nuclear Instruments and Methods in Physics Research Section A: Accelerators, Spectrometers, Detectors and Associated Equipment* **2014**, 736, 66–74. <https://doi.org/https://doi.org/10.1016/j.nima.2013.09.060>.
14. B. Jiang et al.. Monte-Carlo calculations of the energy resolution function with Geant4 for analyzing the neutron capture cross section of ^{232}Th measured at CSNS Back-n. *Nuclear Instruments and Methods in Physics Research Section A: Accelerators, Spectrometers, Detectors and Associated Equipment* **2021**, 1013, 165677. <https://doi.org/https://doi.org/10.1016/j.nima.2021.165677>.
15. Guerrero, C.; Tsinganis, A.; Berthoumieux, E.; Barbagallo, M.; Belloni, F.; Günsing, F.; Weiß, C.; Chiaveri, E.; Calviani, M.; Vlachoudis, V.; et al. Performance of the neutron time-of-flight facility n_TOF at CERN. *European Physical Journal A* **2013**, 49, 27. <https://doi.org/10.1140/epja/i2013-13027-6>.
16. Pavón-Rodríguez, J.A.; Leredegui-Marco, J.; Manna, A.;; n_TOF Collaboration, T. Characterisation of the neutron beam in the n_TOF-EAR2 experimental area at CERN following the spallation target upgrade. *The European Physical Journal A* **2025**, 61, 277. <https://doi.org/10.1140/epja/s10050-025-01727-x>.
17. Guerrero, C.; Domingo-Pardo, C.; Käppeler, F.; Leredegui-Marco, J.; Palomo, F.R.; Quesada, J.M.; Reifarth, R. Prospects for direct neutron capture measurements on s-process branching point isotopes. *The European Physical Journal A* **2017**, 53, 87. <https://doi.org/10.1140/epja/i2017-12261-2>.
18. Wallner, A.; Bichler, M.; Buczak, K.; Dillmann, I.; Käppeler, F.; Karakas, A.; Lederer, C.; Lugaro, M.; Mair, K.; Mengoni, A.; et al. Accelerator mass spectrometry measurements of the $^{13}\text{C}(n, \gamma)^{14}\text{C}$ and $^{14}\text{N}(n, p)^{14}\text{C}$ cross sections. *Phys. Rev. C* **2016**, 93, 045803. <https://doi.org/10.1103/PhysRevC.93.045803>.
19. Reifarth, R.; Arlandini, C.; Heil, M.; Käppeler, F.; Sedyshev, P.V.; Mengoni, A.; Herman, M.; Rauscher, T.; Gallino, R.; Travaglio, C. Stellar Neutron Capture on Promethium: Implications for the s-Process Neutron Density. *The Astrophysical Journal* **2003**, 582, 1251. <https://doi.org/10.1086/344718>.
20. Paul, M.; Tessler, M.; Friedman, M.; Halfon, S.; Palchan, T.; Weissman, L.; Arenshtam, A.; Berkovits, D.; Eisen, Y.; Eliahu, I.; et al. Reactions along the astrophysical s-process path and prospects for neutron radiotherapy with the Liquid-Lithium Target (LiLiT) at the Soreq Applied Research Accelerator Facility (SARAF). *The European Physical Journal A* **2019**, 55, 44. <https://doi.org/10.1140/epja/i2019-12723-5>.
21. Millán-Callado, M.; Guerrero, C.; Fernández, B.; Gómez-Camacho, J.; Macías, M.; Quesada, J. Continuous and pulsed fast neutron beams at the CNA HiSPANoS facility. *Radiation Physics and Chemistry* **2024**, 217, 111464. <https://doi.org/https://doi.org/10.1016/j.radphyschem.2023.111464>.
22. Mastinu, P.; Praena, J.; Martín-Hernández, G.; Dzysiuk, N.; Prete, G.; Capote, R.; Pignatari, M.; Ventura, A. Status of the LEgnaro NeutrOn Source facility (LENOS). *Physics Procedia* **2012**, 26, 261–273. Proceedings of the first two meetings of the Union of Compact Accelerator-Driven Neutron Sources, <https://doi.org/https://doi.org/10.1016/j.phpro.2012.03.034>.
23. Guerrero, C.; Leredegui-Marco, J.; Paul, M.; Tessler, M.; Heinitz, S.; Domingo-Pardo, C.; Cristallo, S.; Dressler, R.; Halfon, S.; Kivel, N.; et al. Neutron Capture on the s-Process Branching Point ^{171}Tm via Time-of-Flight and Activation. *Phys. Rev. Lett.* **2020**, 125, 142701. <https://doi.org/10.1103/PhysRevLett.125.142701>.
24. Musacchio-González, E.; Mastinu, P.; Martín-Hernández, G.; Porras, I.; Centofante, L.; Arias de Saavedra, F.; Maran, L.; Ruzzon, A.; Lideo, D. Maxwell-Boltzmann-like neutron spectrum production for Maxwellian averaged cross sections measurements. *Nuclear Instruments and Methods in Physics Research Section A: Accelerators, Spectrometers, Detectors and Associated Equipment* **2024**, 1063, 169255. <https://doi.org/https://doi.org/10.1016/j.nima.2024.169255>.
25. Praena, J.; Verdera, A.; López, J.G.; Martín-Hernández, G. Production and measurement of a stellar neutron spectrum at 30 keV. *The European Physical Journal A* **2024**, 60, 199. <https://doi.org/10.1140/epja/s10050-024-01404-5>.
26. Heftrich, Tanja.; Al-Khasawleh, Kafa.; Borzek, Sandra.; Brückner, Benjamin.; Dellmann, Sophia Florence.; Dogan, Ozan Can.; El Mard, Asmaa.; Erbacher, Philipp.; Gail, Madeleine.; Göbel, Kathrin.; et al. Neutron activations for lower s-process temperatures. *EPJ Web Conf.* **2023**, 279, 06011. <https://doi.org/10.1051/epjconf/202327906011>.
27. Pérez-Maroto, P.; Guerrero, C.; Casanovas, A.; Fernández, B.; Aberle, O.; Alcayne, V.; Altieri, S.; Amaducci, S.; Andrzejewski, J.; Babiano-Suarez, V.; et al. Description and outlook of the $^{50,53}\text{Cr}(n, \gamma)$ cross section measurement at n_TOF and HiSPANoS. *EPJ Web of Conf.* **2024**, 294, 01004. <https://doi.org/10.1051/epjconf/202429401004>.
28. Patronis, N.; Mengoni, A.; Colonna, N.; Cecchetto, M.; Leredegui-Marco, J.; Aberle, O.; Domingo-Pardo, C.; Gervino, G.; Stamati, M.E.; Goula, S.; et al. The CERN n_TOF NEAR station for astrophysics- and application-related neutron activation measurements. *The European Physical Journal A* **2025**, 61, 215. <https://doi.org/10.1140/epja/s10050-025-01674-7>.

29. Lederer, C.; et al. n_ACT@BDF: A Neutron Activation Station at the SPS Beam Dump Facility (BDF) 2025.
30. Domingo-Pardo, C.; Babiano-Suarez, V.; Balibrea-Correa, J.; Caballero, L.; Ladarescu, I.; Leredegui-Marco, J.; Tain, J.L.; Tarifeño-Saldivia, A.; Aberle, O.; Alcayne, V.; et al. Advances and new ideas for neutron-capture astrophysics experiments at CERN n_TOF. *The European Physical Journal A* **2023**, *59*, 8. <https://doi.org/10.1140/epja/s10050-022-00876-7>.
31. Leredegui-Marco, J.; Guerrero, C.; Domingo-Pardo, C.; Casanovas, A.; Dressler, R.; Halfon, S.; Heinitz, S.; Kivel, N.; Köster, U.; Paul, M.; et al. Measuring neutron capture rates on ILL-produced unstable isotopes (^{147}Pm , ^{171}Tm and ^{204}Tl , and plans for ^{79}Se and ^{163}Ho) for nucleosynthesis studies. *EPJ Web Conf.* **2018**, *193*, 04007. <https://doi.org/10.1051/epjconf/201819304007>.
32. McKay, J.E.; Denissenkov, P.A.; Herwig, F.; Perdikakis, G.; Schatz, H. The impact of (n,γ) reaction rate uncertainties on the predicted abundances of i-process elements. *Monthly Notices of the Royal Astronomical Society* **2019**, *491*, 5179–5187. <https://doi.org/10.1093/mnras/stz3322>.
33. Denissenkov, P.A.; Herwig, F.; Perdikakis, G.; Schatz, H. The impact of (n,γ) reaction rate uncertainties of unstable isotopes on the i-process nucleosynthesis of the elements from Ba to W. *Monthly Notices of the Royal Astronomical Society* **2021**, *503*, 3913–3925, [<https://academic.oup.com/mnras/article-pdf/503/3/3913/36856479/stab772.pdf>]. <https://doi.org/10.1093/mnras/stab772>.
34. Martinet, Sébastien.; Choplin, Arthur.; Goriely, Stéphane.; Siess, Lionel. The intermediate neutron capture process - IV. Impact of nuclear model and parameter uncertainties. *A&A* **2024**, *684*, A8. <https://doi.org/10.1051/0004-6361/202347734>.
35. Choplin, A.; Siess, L.; Goriely, S. The intermediate neutron capture process - I. Development of the i-process in low-metallicity low-mass AGB stars. *Astronomy & Astrophysics* **2021**, *648*, A119. <https://doi.org/10.1051/0004-6361/202040170>.
36. Weiß, C.; Chiaveri, E.; Girod, S.; Vlachoudis, V.; Aberle, O.; Barros, S.; Bergström, I.; Berthoumieux, E.; Calviani, M.; Guerrero, C.; et al. The new vertical neutron beam line at the CERN n_TOF facility design and outlook on the performance. *Nuclear Instruments and Methods in Physics Research Section A: Accelerators, Spectrometers, Detectors and Associated Equipment* **2015**, *799*, 90–98. <https://doi.org/https://doi.org/10.1016/j.nima.2015.07.027>.
37. Guerrero, C.; Abbondanno, U.; Aerts, G.; Álvarez, H.; Álvarez Velarde, F.; Andriamonje, S.; Andrzejewski, J.; Assimakopoulos, P.; Audouin, L.; Badurek, G.; et al. The n_TOF Total Absorption Calorimeter for neutron capture measurements at CERN. *Nuclear Instruments and Methods in Physics Research Section A: Accelerators, Spectrometers, Detectors and Associated Equipment* **2009**, *608*, 424–433. <https://doi.org/https://doi.org/10.1016/j.nima.2009.07.025>.
38. Plag, R.; Heil, M.; Käppeler, F.; Pavlopoulos, P.; Reifarth, R.; Wisshak, K.; n_TOF Collaboration. An optimized $^6\text{D}_6$ detector for studies of resonance-dominated (n,γ) cross-sections. *Nuclear Instruments and Methods in Physics Research A* **2003**, *496*, 425–436. [https://doi.org/10.1016/S0168-9002\(02\)01749-7](https://doi.org/10.1016/S0168-9002(02)01749-7).
39. Tain, J.; Günsing, F.; Aniel-Cano, D.; Nicola, C.; Domingo, C.; Gonzalez, E.; Heil, M.; Käppeler, F.; Makrone, S.; Mastinu, P.; et al. Accuracy of the pulse height weighting technique for capture cross section measurements. *Journal of Nuclear Science and Technology* **2002**, *39*, 689–692. <https://doi.org/10.1080/00223131.2002.10875193>.
40. Abbondanno, U.; Aerts, G.; Alvarez, H.; Andriamonje, S.; Angelopoulos, A.; Assimakopoulos, P.; Bacri, C.O.; Badurek, G.; Baumann, P.; Bečvář, F.; et al. New experimental validation of the pulse height weighting technique for capture cross-section measurements. *Nuclear Instruments and Methods in Physics Research A* **2004**, *521*, 454–467. <https://doi.org/10.1016/j.nima.2003.09.066>.
41. Moxon, M.C.; Rae, E.R. A gamma-ray detector for neutron capture cross-section measurements. *Nuclear Instruments and Methods* **1963**, *24*, 445–455. [https://doi.org/10.1016/0029-554X\(63\)90364-1](https://doi.org/10.1016/0029-554X(63)90364-1).
42. Leredegui-Marco, J.; Guerrero, C.; Mendoza, E.; Quesada, J.M.; Eberhardt, K.; Junghans, A.R.; Krtička, M.; Aberle, O.; Andrzejewski, J.; Audouin, L.; et al. Radiative neutron capture on ^{242}Pu in the resonance region at the CERN n_TOF-EAR1 facility. *Physical Review C* **2018**, *97*, 024605. <https://doi.org/10.1103/PhysRevC.97.024605>.
43. Babiano, V.; et al. First high-resolution $^{80}\text{Se}(n,\gamma)$ cross section measurement between 1 eV and 100 keV and its astrophysical implications for the s-process. 2022, Vol. ND2022 Conference, *European Physical Journal Web of Conferences*.
44. Aerts, G.; Abbondanno, U.; Álvarez, H.; Alvarez-Velarde, F.; Andriamonje, S.; Andrzejewski, J.; Assimakopoulos, P.; Audouin, L.; Badurek, G.; Baumann, P.; et al. Neutron capture cross section of ^{232}Th measured at the n_TOF facility at CERN in the unresolved resonance region up to 1 MeV. *Phys. Rev. C* **2006**, *73*, 054610. <https://doi.org/10.1103/PhysRevC.73.054610>.
45. Lederer, C.; Colonna, N.; Domingo-Pardo, C.; Günsing, F.; Käppeler, F.; Massimi, C.; Mengoni, A.; Wallner, A.; Abbondanno, U.; Aerts, G.; et al. $^{197}\text{Au}(n,\gamma)$ cross section in the unresolved resonance region. *Phys. Rev. C* **2011**, *83*, 034608. <https://doi.org/10.1103/PhysRevC.83.034608>.
46. Mingrone, F.; Massimi, C.; Vannini, G.; Colonna, N.; Günsing, F.; Žugec, P.; Altstadt, S.; Andrzejewski, J.; Audouin, L.; Barbagallo, M.; et al. Neutron capture cross section measurement of ^{238}U at the CERN n_TOF facility in the energy region from 1 eV to 700 keV. *Phys. Rev. C* **2017**, *95*, 034604. <https://doi.org/10.1103/PhysRevC.95.034604>.
47. Leredegui-Marco, J.; Collaboration, T.n. Radiative neutron capture cross section of ^{242}Pu measured at n_TOF-EAR1 in the unresolved resonance region up to 600 keV. *The European Physical Journal A* **2026**, *63*. <https://doi.org/10.1140/epja/s10050-026-01788-6>.

48. Milazzo, P.M.; Lederer-Woods, C.; Mengoni, A. The Nuclear Astrophysics Program at the CERN n_TOF Facility: Results and Perspectives. *Universe* **2025**, *11*. <https://doi.org/10.3390/universe11100329>.
49. Mazzone, A.; Cristallo, S.; Aberle, O.; Measurement of the $^{154}\text{Gd}(n,\gamma)$ cross section and its astrophysical implications. *Physics Letters B* **2020**, *804*, 135405. <https://doi.org/10.1016/j.physletb.2020.135405>.
50. Straniero, O.; Cristallo, S.; Piersanti, L. Heavy Elements in Globular Clusters: The Role of Asymptotic Giant Branch Stars. *The Astrophysical Journal* **2014**, *785*, 77. <https://doi.org/10.1088/0004-637X/785/1/77>.
51. Domingo-Pardo, C.; Abbondanno, U.; Aerts, G.; Álvarez-Pol, H.; Alvarez-Velarde, F.; Andriamonje, S.; Andrzejewski, J.; Assimakopoulos, P.; Audouin, L.; Badurek, G.; et al. Resonance capture cross section of ^{207}Pb . *Phys. Rev. C* **2006**, *74*, 055802. <https://doi.org/10.1103/PhysRevC.74.055802>.
52. Domingo-Pardo, C.; Abbondanno, U.; Aerts, G.; Álvarez-Pol, H.; Alvarez-Velarde, F.; Andriamonje, S.; Andrzejewski, J.; Assimakopoulos, P.; Audouin, L.; Badurek, G.; et al. New measurement of neutron capture resonances in Bi209. *Physical Review C* **2006**, *74*, 025807. <https://doi.org/10.1103/PhysRevC.74.025807>.
53. Balibrea-Correa, J.; et al.. High precision $^{209}\text{Bi}(n,\gamma)$ cross section measurement at n TOF EAR2. *CERN-INTC-2023-061 / INTC-P-675* **2023**.
54. Romojaro, P.; Paradela Dobarro, C.; Alaerts, G.; L., F.; Heyse, J.; Kopecky, S.; Moscati, S.; Schillebeeckx, P.; Stankovskiy, A.; Van Den Eynde, G.; et al. Results of time-of-flight transmission measurements for 209Bi at a 50 m station of GELINA **2024**. [https://doi.org/10.2760/02812\(online\)](https://doi.org/10.2760/02812(online)).
55. Richter, S.; Ott, U.; Begemann, F. S-Process Isotope Anomalies: Neodymium, Samarium, and a Bit More of Strontium. In Proceedings of the Lunar and Planetary Science Conference, 1992, Vol. 23, *Lunar and Planetary Science Conference*, p. 1147.
56. Liu, N. Isotopic compositions of s-process elements in acid-cleaned mainstream presolar silicon carbide. PhD thesis, United States – Illinois, 2014. Copyright - Database copyright ProQuest LLC; ProQuest does not claim copyright in the individual underlying works.
57. Vescovi, Diego.; Reifarh, René.; Lorenz, Enis.; Elbe, Andreas. The ASTRAL database for neutron-capture nucleosynthesis studies. *EPJ Web Conf.* **2023**, *279*, 11011. <https://doi.org/10.1051/epjconf/202327911011>.
58. Yin, Q.Z.; Lee, C.T.A.; Ott, U. Signatures of the s-Process in Presolar Silicon Carbide Grains: Barium through Hafnium. *The Astrophysical Journal* **2006**, *647*, 676 – 684.
59. Cristallo, S.; Straniero, O.; Piersanti, L.; Gobrecht, D. EVOLUTION, NUCLEOSYNTHESIS, AND YIELDS OF AGB STARS AT DIFFERENT METALLICITIES. III. INTERMEDIATE-MASS MODELS, REVISED LOW-MASS MODELS, AND THE pH-FRUITY INTERFACE. *The Astrophysical Journal Supplement Series* **2015**, *219*, 40. <https://doi.org/10.1088/0067-0049/219/2/40>.
60. Wisshak, K.; Voss, F.; Käppeler, F.; Kazakov, L.; Reffo, G. Stellar neutron capture cross sections of the Nd isotopes. *Phys. Rev. C* **1998**, *57*, 391–408. <https://doi.org/10.1103/PhysRevC.57.391>.
61. Lerendegui-Marco, J.; et al.. New measurement of the $^{146}\text{Nd}(n,\gamma)$ cross section at n TOF-EAR2. 2023, CERN-INTC-2023-055 / INTC-P-671.
62. Gameiro, B.; Lerendegui-Marco, J.; et al.. Measurement of the $^{146}\text{Nd}(n,\gamma)$ MACS at s-process stellar temperatures at n TOF-NEAR. 2025, CERN-INTC-2025-044 / INTC-P-671-ADD-1.
63. Lerendegui-Marco, J.; Casanovas, A.; Alcayne, V.; Aberle, O.; Altieri, S.; Amaducci, S.; Andrzejewski, J.; Babiano-Suarez, V.; Bacak, M.; Balibrea, J.; et al. New perspectives for neutron capture measurements in the upgraded CERN-n_TOF Facility. *EPJ Web of Conf.* **2023**, *284*, 01028. <https://doi.org/10.1051/epjconf/202328401028>.
64. Mastinu, P. New C_6D_6 detectors: reduced neutron sensitivity and improved safety. n_tof-pub-2013-002 26/06/2013, CERN n_TOF Collaboration, 2013. n_TOF-PUB-2013-002 26/06/2013.
65. Domingo-Pardo, C. i-TED: A novel concept for high-sensitivity (n,γ) cross-section measurements. *Nuclear Instruments and Methods in Physics Research A* **2016**, *825*, 78–86. <https://doi.org/10.1016/j.nima.2016.04.002>.
66. Babiano, V.; Lerendegui-Marco, J.; et al.. Imaging neutron capture cross sections: i-TED proof-of-concept and future prospects based on Machine-Learning techniques. *The European Physical Journal A* **2021**, *57*, 197.
67. Alcayne, V.; Cano-Ott, D.; Garcia, J.; González-Romero, E.; Martínez, T.; de Rada, A.P.; Plaza, J.; Sánchez-Caballero, A.; Balibrea-Correa, J.; Domingo-Pardo, C.; et al. A Segmented Total Energy Detector (sTED) optimized for (n,γ) cross-section measurements at n_TOF EAR2. *Radiation Physics and Chemistry* **2024**, *217*, 111525. <https://doi.org/https://doi.org/10.1016/j.radphyschem.2024.111525>.
68. Balibrea-Correa, J.; Babiano-Suarez, V.; Lerendegui-Marco, J.; Domingo-Pardo, C.; Ladarescu, I.; Tarifeño-Saldivia, A.; Towards a new generation of solid total-energy detectors for neutron-capture time-of-flight experiments with intense neutron beams. *Nuclear Instruments and Methods in Physics Research Section A* **2025**, *1072*, 170110. <https://doi.org/10.1016/j.nima.2024.170110>.
69. Abbondanno, U.; Aerts, G.; Alvarez-Velarde, F.; Álvarez-Pol, H.; Andriamonje, S.; Andrzejewski, J.; Badurek, G.; Baumann, P.; Bečvář, F.; Benlliure, J.; et al. Neutron Capture Cross Section Measurement of ^{151}Sm at the CERN Neutron Time of Flight Facility (n_TOF). *Phys. Rev. Lett.* **2004**, *93*, 161103. <https://doi.org/10.1103/PhysRevLett.93.161103>.

70. Tagliente, G.; Milazzo, P.M.; Fujii, K.; Abbondanno, U.; Aerts, G.; Álvarez, H.; Alvarez-Velarde, F.; Andriamonje, S.; Andrzejewski, J.; Audouin, L.; et al. The $^{93}\text{Zr}(n, \gamma)$ reaction up to 8 keV neutron energy. *Phys. Rev. C* **2013**, *87*, 014622. <https://doi.org/10.1103/PhysRevC.87.014622>.
71. Lederer, C.; Massimi, C.; Altstadt, S.; Andrzejewski, J.; Audouin, L.; Barbagallo, M.; Bécáres, V.; Bečvář, F.; Belloni, F.; Berthoumieux, E.; et al. Neutron Capture Cross Section of Unstable ^{63}Ni : Implications for Stellar Nucleosynthesis. *Phys. Rev. Lett.* **2013**, *110*, 022501. <https://doi.org/10.1103/PhysRevLett.110.022501>.
72. Casanovas-Hoste, A.; Domingo-Pardo, C.; Lerendegui-Marco, J.; Guerrero, C.; Tarifeño Saldivia, A.; Krtička, M.; Pignatari, M.; Shedding Light on the Origin of ^{204}Pb , the Heaviest s-Process-Only Isotope in the Solar System. *Phys. Rev. Lett.* **2024**, *133*, 052702. <https://doi.org/10.1103/PhysRevLett.133.052702>.
73. Lerendegui-Marco, J.; Lo Meo, S.; Guerrero, C.; Cortés-Giraldo, M.A.; Massimi, C.; Quesada, J.M.; Barbagallo, M.; Colonna, N.; Mancusi, D.; Mingrone, F.; et al. Geant4 simulation of the n_TOF-EAR2 neutron beam: Characteristics and prospects. *European Physical Journal A* **2016**, *52*, 100. <https://doi.org/10.1140/epja/i2016-16100-8>.
74. Esposito, R.; Calviani, M.; Aberle, O.; Barbagallo, M.; Cano-Ott, D.; Coiffet, T.; Colonna, N.; Domingo-Pardo, C.; Dragoni, F.; Franqueira Ximenes, R.; et al. Design of the third-generation lead-based neutron spallation target for the neutron time-of-flight facility at CERN. *Phys. Rev. Accel. Beams* **2021**, *24*, 093001. <https://doi.org/10.1103/PhysRevAccelBeams.24.093001>.
75. Bacak, M.; et al.. Characterisation of the n_TOF/CERN 185m beam-line after the facility's major upgrades . 2022, Vol. ND2022 Conference, *European Physical Journal Web of Conferences*.
76. Pavón, J.A.; et al.. Characterisation of the n_TOF 20 m beam line at CERN with the new spallation target. 2022, Vol. ND2022 Conference, *European Physical Journal Web of Conferences*.
77. Lerendegui-Marco, J.; Babiano-Suárez, V.; Balibrea-Correa, J.; Domingo-Pardo, C.; Ladarescu, I.; Tarifeño-Saldivia, A.; Alcayne, V.; Cano-Ott, D.; González-Romero, E.; Martínez, T.; et al. New detection systems for an enhanced sensitivity in key stellar (n,asurements. *EPJ Web Conf.* **2023**, *279*, 13001. <https://doi.org/10.1051/epjconf/202327913001>.
78. Balibrea-Correa, J.; Babiano-Suárez, V.; Lerendegui-Marco, J.; Domingo-Pardo, C.; Ladarescu, I.; Tarifeño-Saldivia, A.; Alcayne, V.; Cano-Ott, D.; González-Romero, E.; Martínez, T.; et al. First measurement of the $^{94}\text{Nb}(n, \text{oss})$ section at the CERN n_TOF facility. *EPJ Web Conf.* **2023**, *279*, 06004. <https://doi.org/10.1051/epjconf/202327906004>.
79. Babiano, V.; Caballero, L.; Calvo, D.; Ladarescu, I.; Olleros, P.; Domingo-Pardo, C. γ -Ray position reconstruction in large monolithic $\text{LaCl}_3(\text{Ce})$ crystals with SiPM readout. *Nuclear Instruments and Methods in Physics Research A* **2019**, *931*, 1–22. <https://doi.org/10.1016/j.nima.2019.03.079>.
80. Babiano, V.; Balibrea, J.; Caballero, L.; Calvo, D.; Ladarescu, I.; Lerendegui, J.; Mira Prats, S.; Domingo-Pardo, C. First i-TED demonstrator: A Compton imager with Dynamic Electronic Collimation. *Nuclear Instruments and Methods in Physics Research A* **2020**, *953*, 163228. <https://doi.org/10.1016/j.nima.2019.163228>.
81. Balibrea-Correa, J.; Lerendegui-Marco, J.; Babiano-Suárez, V.; Caballero, L.; Calvo, D.; Ladarescu, I.; Olleros-Rodríguez, P.; Domingo-Pardo, C. Machine Learning aided 3D-position reconstruction in large LaCl_3 crystals. *Nuclear Instruments and Methods in Physics Research Section A: Accelerators, Spectrometers, Detectors and Associated Equipment* **2021**, *1001*, 165249. <https://doi.org/https://doi.org/10.1016/j.nima.2021.165249>.
82. Lerendegui-Marco, J.; Babiano-Suárez, V.; Balibrea-Correa, J.; Babiano-Suárez, V.; Caballero, L.; Calvo, D.; Domingo-Pardo, C.; Ladarescu, I.; Real, D.; Calviño, F.; et al. Compton Imaging and Machine-Learning techniques for an enhanced sensitivity in key stellar (n,asurements. *EPJ Web Conf.* **2022**, *260*, 10002. <https://doi.org/10.1051/epjconf/202226010002>.
83. Balibrea-Correa, J. "First $^{94}\text{Nb}(n, \gamma)$ Branching Point Cross Section Measurement: Implications for AGB Presolar Grains. *Phys. Rev. Lett.* **2026**, (submitted).
84. Chiera, N.M.; Maugeri, E.A.; Danilov, I.; Balibrea-Correa, J.; Domingo-Pardo, C.; Köster, U.; Lerendegui-Marco, J.; Veicht, M.; Zivadinovic, I.; Schumann, D. Preparation of PbSe targets for ^{79}Se neutron capture cross section studies. *Nuclear Instruments and Methods in Physics Research Section A: Accelerators, Spectrometers, Detectors and Associated Equipment* **2022**, *1029*, 166443. <https://doi.org/https://doi.org/10.1016/j.nima.2022.166443>.
85. Casanovas, A.; Tarifeño-Saldivia, A.E.; Domingo-Pardo, C.; Calviño, F.; Maugeri, E.; Guerrero, C.; Lerendegui-Marco, J.; Dressler, R.; Heinitz, S.; Schumann, D.; et al. Neutron capture measurement at the n TOF facility of the ^{204}Tl and ^{205}Tl s-process branching points. *Journal of Physics: Conference Series* **2020**, *1668*, 012005. <https://doi.org/10.1088/1742-6596/1668/1/012005>.
86. Alcayne, V.; et al.. Results of the ^{244}Cm , ^{246}Cm and ^{248}Cm neutron-induced capture cross sections measurements at EAR1 and EAR2 of the n_TOF facility. 2022, Vol. ND2022 Conference, *European Physical Journal Web of Conferences*.
87. Guerrero, C.; Tessler, M.; Paul, M.; Lerendegui-Marco, J.; Heinitz, S.; Maugeri, E.; Domingo-Pardo, C.; Dressler, R.; Halfon, S.; Kivel, N.; et al. The s-process in the Nd-Pm-Sm region: Neutron activation of ^{147}Pm . *Physics Letters B* **2019**, *797*, 134809. <https://doi.org/https://doi.org/10.1016/j.physletb.2019.134809>.
88. Lerendegui-Marco, J.; Alcayne, V.; Babiano-Suarez, V.; Bacak, M.; Balibrea-Correa, J.; Casanovas, A.; Domingo-Pardo, C.; de la Fuente, G.; Gameiro, B.; García-Infantes, F.; et al. Recent highlights and prospects on (n, γ) measurements at the CERN n_TOF facility. *EPJ Web Conf.* **2025**, *329*, 03003. <https://doi.org/10.1051/epjconf/202532903003>.

89. Leredegui-Marco, J.; Domingo-Pardo, C.; et al.. First measurement of the s-process branching $^{79}\text{Se}(n,\gamma)$. *CERN-INTC-2020-065;INTC-P-580* **2020**.
90. Schumann, D.; Ayranov, M.; Dressler, R.. Achievements and perspectives of ERAWAST. *EPJ Web of Conferences* **2010**, *8*, 05003. <https://doi.org/10.1051/epjconf/20100805003>.
91. Leredegui-Marco, J.; Bacak, M.; et al.. Towards an optimized experimental setup for future neutron capture measurements at n_TOF-EAR2. 2023, CERN-INTC-2023-036; INTC-P-587-ADD-1.
92. Bacak, M.; Casanovas, A.; et al.. Towards reducing the neutron background for n,g) measurements at n TOF-EAR2. 2025, CERN-INTC-2025-042 / INTC-P-587-ADD-2.
93. Mendoza, E.; Alcayne, V.; Cano-Ott, D.; González-Romero, E.; Martínez, T.; Pérez de Rada, A.; Sánchez-Caballero, A.; Balibrea-Correa, J.; Domingo-Pardo, C.; Leredegui-Marco, J.; et al. Neutron capture measurements with high efficiency detectors and the Pulse Height Weighting Technique. *Nuclear Instruments and Methods in Physics Research Section A: Accelerators, Spectrometers, Detectors and Associated Equipment* **2023**, *1047*, 167894. <https://doi.org/https://doi.org/10.1016/j.nima.2022.167894>.
94. Stamati, E.; et al.. The n_TOF NEAR Station: Physics case and commissioning. 2022, Vol. ND2022 Conference, *European Physical Journal Web of Conferences*.
95. Aberle, O. n_TOF Technical Report. *81st Meeting of the INTC* **2026**.
96. Leredegui-Marco, J.; Carollo, S.; et al.. Activation measurements of the $^{135}\text{Cs}(n,\gamma)$ cross-section at n_TOF-NEAR. 2024, CERN-INTC-2024-007 / INTC-P-690.
97. Taioli, S.; Vescovi, D.; Busso, M.; Palmerini, S.; Cristallo, S.; Mengoni, A.; Simonucci, S. Theoretical Estimate of the Half-life for the Radioactive ^{134}Cs and ^{135}Cs in Astrophysical Scenarios. *The Astrophysical Journal* **2022**, *933*, 158. <https://doi.org/10.3847/1538-4357/ac74b3>.
98. Palmerini, S.; Busso, M.; Vescovi, D.; Naselli, E.; Pidatella, A.; Mucciola, R.; Cristallo, S.; Mascali, D.; Mengoni, A.; Simonucci, S.; et al. Presolar Grain Isotopic Ratios as Constraints to Nuclear and Stellar Parameters of Asymptotic Giant Branch Star Nucleosynthesis. *The Astrophysical Journal* **2021**, *921*, 7. <https://doi.org/10.3847/1538-4357/ac1786>.
99. Patronis, N.; Dababneh, S.; Assimakopoulos, P.A.; Gallino, R.; Heil, M.; Käppeler, F.; Karamanis, D.; Koehler, P.E.; Mengoni, A.; Plag, R. Neutron capture studies on unstable ^{135}Cs for nucleosynthesis and transmutation. *Phys. Rev. C* **2004**, *69*, 025803. <https://doi.org/10.1103/PhysRevC.69.025803>.
100. Leredegui-Marco, J.; Carollo, S.; et al.. Production of a ^{135}Cs sample at ISOLDE for (n,γ) activation measurements at n_TOF-NEAR. 2023, INTC-2023-036; INTC-P-587-ADD-1.
101. Leredegui-Marco, J.; Bacak, M.; et al.. Measurement of the radiation background at the n_TOF NEAR facility to study the feasibility of cyclic activation experiments. Technical report, 2022.
102. The fast cyclic neutron activation technique at the Karlsruhe 3.75 MV Van de Graaff accelerator and the measurement of the $^{107,109}\text{Ag}(n,\gamma)^{108,110}\text{Ag}$ cross sections at $kT = 25$ keV. *Nuclear Instruments and Methods in Physics Research Section A: Accelerators, Spectrometers, Detectors and Associated Equipment* **1994**, *337*, 492–503.
103. Ibarra, A.; Królas, W.; Bernardi, D.; Cano-Ott, D.; Becerril-Jarque, S.; Álvarez, I.; Qiu, Y.; the EUROfusion WPENS Team. DONES performance, experimental capabilities and perspectives. *Nuclear Fusion* **2025**, *65*, 122006. <https://doi.org/10.1088/1741-4326/adcd86>.
104. Reifarh, R.; Litvinov, Y.A. Measurements of neutron-induced reactions in inverse kinematics. *Phys. Rev. ST Accel. Beams* **2014**, *17*, 014701. <https://doi.org/10.1103/PhysRevSTAB.17.014701>.
105. Reifarh, R.; Göbel, K.; Heftrich, T.; Weigand, M.; Jurado, B.; Käppeler, F.; Litvinov, Y.A. Spallation-based neutron target for direct studies of neutron-induced reactions in inverse kinematics. *Phys. Rev. Accel. Beams* **2017**, *20*, 044701. <https://doi.org/10.1103/PhysRevAccelBeams.20.044701>.
106. Tarifeño-Saldivia, A.; Domingo-Pardo, C.; Dillmann, I.; Litvinov, Y.A. Direct Neutron Reactions in Storage Rings Utilizing a Supercompact Cyclotron Neutron Target. *Phys. Rev. Accel. Beams (submitted)* **2026**, [arXiv:nucl-ex/2508.15465].
107. Grieser, M.; Litvinov, Y.A.; Raabe, R.; Blaum, K.; Blumenfeld, Y.; Butler, P.A.; Wenander, F.; Woods, P.J.; Aliotta, M.; Andreyev, A.; et al. Storage ring at HIE-ISOLDE. *The European Physical Journal Special Topics* **2012**, *207*, 1–117. <https://doi.org/10.1140/epjst/e2012-01599-9>.

Disclaimer/Publisher’s Note: The statements, opinions and data contained in all publications are solely those of the individual author(s) and contributor(s) and not of MDPI and/or the editor(s). MDPI and/or the editor(s) disclaim responsibility for any injury to people or property resulting from any ideas, methods, instructions or products referred to in the content.